Calhoun: The NPS Institutional Archive

DSpace Repository

Theses and Dissertations | 1. Thesis and Dissertation Collection, all items

1991-09

A design, fabrication and test of a precision positioning servo drive for a multiplexed imaging system

Sargent, Joseph Patrick

Monterey, California. Naval Postgraduate School

https://hdl.handle.net/10945/26449

Downloaded from NPS Archive: Calhoun

http://www.nps.edu/library

Calhoun is the Naval Postgraduate School's public access digital repository for research materials and institutional publications created by the NPS community. Calhoun is named for Professor of Mathematics Guy K. Calhoun, NPS's first appointed -- and published -- scholarly author.

Dudley Knox Library / Naval Postgraduate School
411 Dyer Road / 1 University Circle
Monterey, California USA 93943

NAVAL POSTGRADUATE SCHOOL

Monterey, California

THESIS

A Design, Fabrication and Test of a Precision Positioning Servo Drive for a Multiplexed Imaging System

by

Joseph Patrick Sargent Jr.

SEPTEMBER 1991

Thesis Advisor: **D. Scott Davis**

APPROVED FOR PUBLIC RELEASE: DISTRIBUTION IS UNLIMITED

REPORT DOCUMENTATION PAGE

Form Approved
OMB No. 0704-0188

1a REPORT SECURITY CLASSIFICATION Unclassified	1b RESTRICTIVE MARKINGS
2a SECURITY CLASSIFICATION AUTHORITY	3 DISTRIBUTION/AVAILABILITY OF REPORT Approved for public release Distribution is unlimited
2b DECLASSIFICATION/DOWNGRADING SCHEDULE	
4 PERFORMING ORGANIZATION REPORT NUMBER(S)	5 MONITORING ORGANIZATION REPORT NUMBER(S)
6a NAME OF PERFORMING ORGANIZATION Navy Postgraduate School 6b OFFICE SYMBOL (If applicable) PH/Dv	7a NAME OF MONITORING ORGANIZATION Naval Postgraduate School
6c ADDRESS (City, State, and ZIP Code) Monterey, CA 93943-5000	7b ADDRESS (City, State, and ZIP Code) Monterey, CA 93943-5000
8a NAME OF FUNDING/SPONSORING ORGANIZATION 8b OFFICE SYMBOL (If applicable)	9 PROCUREMENT INSTRUMENT IDENTIFICATION NUMBER
8c ADDRESS (City, State, and ZIP Code)	10 SOURCE OF FUNDING NUMBERS PROGRAM ELEMENT NO / PROJECT NO / TASK NO / WORK UNIT ACCESSION NO

11 TITLE (Include Security Classification)
A DESIGN, FABRICATION AND TEST OF A PRECISION POSITIONING SERVO DRIVE FOR A MULTIPLEXED IMAGING SYSTEM

12 PERSONAL AUTHOR(S)
JOSEPH PATRICK SARGENT JR.

13a TYPE OF REPORT	13b TIME COVERED	14 DATE OF REPORT (Year, Month, Day)	15 PAGE COUNT
Master's Thesis	FROM _____ TO _____	SEPTEMBER 1991	101

16 SUPPLEMENTARY NOTATION
The views expressed in this thesis are those of the author and do not reflect the official policy or position of the Department of Defense or U.S. Government

17 COSATI CODES			18 SUBJECT TERMS (Continue on reverse if necessary and identify by block number)
FIELD	GROUP	SUB-GROUP	Control System; Servo Drive; Infrared Imaging; DC Motor Theory

19 ABSTRACT (Continue on reverse if necessary and identify by block number)

In support of the development of a new initiative in the field of multiplexed image spectroscopy, a high torque, servo system was developed. Utilizing only a low resolution shaft position encoder, the system demonstrated an excellent ability to track a pulse input signal with high precision and stability. Ultimately, this servo system will be incorporated into a new generation of multiplexed imaging and imaging spectroscopy instruments. It will provide those instruments with the capability to accurately rotate into position a sequence of optical image encoding masks and it will tightly control that position, even in the presence of external perterbations. A computer will read the light intensity signals from a sensor and quick decode the image for viewing and analysis. Further research into this technology should lead to full development of an extremely efficient infrared imaging

20 DISTRIBUTION/AVAILABILITY OF ABSTRACT ☒ UNCLASSIFIED/UNLIMITED ☐ SAME AS RPT ☐ DTIC USERS	21 ABSTRACT SECURITY CLASSIFICATION unclassified
22a NAME OF RESPONSIBLE INDIVIDUAL D. Scott Davis	22b TELEPHONE (Include Area Code) (408) 646-2116 22c OFFICE SYMBOL PH/Dv

DD Form 1473, JUN 86 *Previous editions are obsolete*
S/N 0102-LF-014-6603

T259156

system, with additional applications to passive surveillance, target signature identification, and airborne infrared astrophysics.

Approved for public release: Distribution is unlimited

A Design, Fabrication and Test of a Precision Positioning Servo Drive for a Multiplexed Imaging System

by

Joseph Patrick Sargent Jr.
Lieutenant, United States Coast Guard
B.S., United States Coast Guard Academy, 1981

Submitted in partial fulfillment of the requirements for the degree of

MASTER OF SCIENCE IN PHYSICS

from the

NAVAL POSTGRADUATE SCHOOL
SEPTEMBER 1991

ABSTRACT

In support of the development of a new initiative in the field of multiplexed image spectroscopy, a high torque, servo system was developed. Utilizing only a low resolution shaft position encoder, the system demonstrated an excellent ability to track a pulse input signal with high precision and stability. Ultimately, this servo system will be incorporated into a new generation of multiplexed imaging and imaging spectroscopy instruments. It will provide those instruments with the capability to accurately rotate into position a sequence of optical image encoding masks and it will tightly control that position, even in the presence of external perturbations. A computer will read the light intensity signals from a sensor and quickly decode the image for viewing and analysis. Further research into this technology should lead to full development of an extremely efficient infrared imaging system, with additional applications to passive surveillance, target signature identification, and airborne infrared astrophysics.

TABLE OF CONTENTS

I. INTRODUCTION 1
A. MOTIVATION 1
B. THESIS GOAL 3

II. NATURE OF THE EXPERIMENT 5
A. SYSTEM OVERVIEW 5
B. SERVO DRIVE REQUIREMENTS 7
1. Frequency Bandwidth 7
2. Torque Considerations 7
3. Friction 8
4. Accuracy 8
5. Stability 8

III. EXPERIMENTAL PROCEDURE 10
A. GENERAL APPROACH 10
B. MATHEMATICAL MODELING OF SYSTEM PERFORMANCE . . 10
1. Background 10
2. Solution of Differential Equation 16
C. SYSTEM DESIGN 21
1. Motor Selection 21
2. Power Operational Amplifier Selection . . . 22
3. Power Supplies 22
4. Cage Design 22
5. Shaft Position Encoder 23
6. Motor - Encoder Coupling 23
7. Encoder Analog Conversion Board 23
8. Amplifier Board 27
9. Motor Driver Power Operational Amplifier . . 29
10. Voltage Regulator Circuit 32
D. SYSTEM ASSEMBLY 33
1. Motor - Encoder Cage Assembly 33
2. Motor - Encoder Mounting 33
3. Assembly of Power Operational Amplifier. . . 35
4. Electronics Prototyping 38
5. System Hardwiring 47
E. SYSTEM TESTING 50
1. Preliminary Prototyping Setup Testing . . . 50
2. Motor Speed Test 56
3. Motor Torque Test 58

IV. SUGGESTIONS FOR FURTHER RESEARCH AND SYSTEM ENHANCEMENTS 60

V. CONCLUSIONS 62
LIST OF REFERENCES 63

APPENDIX A - MathCAD Analysis 64

APPENDIX B - DC Motor Catalog Specification 67

APPENDIX C - LM12 Power Op Amp Data Sheet 68

APPENDIX D - 24VDC Power Supply Data Sheet 70

APPENDIX E - Motor-Encoder Enclosure Mechanical Drawing 71

APPENDIX F - Shaft Encoder Catalog Specification . . . 72

APPENDIX G - Motor-Encoder Coupling Mech. Dwg. 73

APPENDIX H - Encoder Analog Conversion Circuit Schematic 74

APPENDIX I - 74LS74 D-type Flip-Flop Data Sheet 75

APPENDIX J - 74LS00 NAND gate Data Sheet 76

APPENDIX K - 74LS193 Up/Down Counter Data Sheet 77

APPENDIX L - DAC0808 Digital-Analog Data Sheet 78

APPENDIX M - Amplifier Circuit Schematic 81

APPENDIX N - LM324 Quad Op Amp Data Sheet 82

APPENDIX O - Motor Power Amp Circuit Schematic 83

APPENDIX P - LM7800 Series Voltage Regulator Data Sheet 84

APPENDIX Q - LM7900 Series Voltage Regulator Data Sheet 85

APPENDIX R - LM301 Operational Amplifier Data Sheet . . 86

APPENDIX S - Low Pass Filter Circuit Schematic 87

APPENDIX T - Differentiator Circuit Schematic 88

APPENDIX U - Encoder DAC Card Layout Drawing 89

APPENDIX V - Feedback Amplifier Card Layout Drawing . . 90

APPENDIX W - Torque Test Bar Mechanical Drawing 91

INITIAL DISTRIBUTION LIST 92

List of Figures

The Proposed Hybrid Multiplexed Imaging-FTS System . . 6
Feedback Control System Block Diagram 12
Electrical circuit model of DC motor 15
Typical dual channel encoder signals in quadrature. . . 25
Photograph of Cage Assembly and Plywood Base 34
Motor-Encoder Shaft Coupling Photograph 36
Photograph of Motor and Encoder Mounted in Cage 37
Photograph of LM12 Op Amp and Heat Sink Assembly . . . 39
Global Specialties Protoboard Model PB-503 40
Photograph of Encoder Analog Conversion Card. 48
Photograph of Amplifier Circuit Card. 49
Photograph of Completed Motor Servo System 51
Photograph of Tektronix Model 2336 Oscilloscope 53
Graph of System Stability vs. Gain 55
Servo Motor Speed Test - Oscilloscope Trace 57
Photograph of Torque Test Setup 59

I. INTRODUCTION

A. MOTIVATION

The development of a new initiative in remote sensing of the spatial and spectral properties of infrared (IR) radiation is the primary motivation for this thesis research. The specific technological discipline is called infrared imaging spectroscopy. The IR wavelength band has been studied for many years. Many types of instrumentation exist for either IR imaging or spectroscopy, but proficient devices that are capable of performing both functions at once are uncommon. Such a hybrid-type of technology should benefit many facets of remote sensing, especially in surveillance/target signature identification as well as in scientific fields of study, like infrared astrophysics.

The author's thesis advisor, D.S. Davis has been the developer of state-of-the-art IR spectroscopic instrumentation for an extended period. He has fielded several infrared spectroscopic devices, one of which is currently deployed aboard NASA's Kuiper Airborne Observatory (KAO).

A proposed successor to the KAO, to be called SOFIA -- Stratospheric Observatory For Infrared Astronomy, is under early stages of development by NASA. SOFIA will be a

modified Boeing 747 jet aircraft carrying a Nasmyth, three meter, open-port telescope supplied by the Federal Republic of Germany. Designed to "address fundamental questions in galactic and extragalactic astronomy and in the origin and evolution of the Solar System" [Ref. 1], Sofia will far surpass the airborne observation capabilities of the KAO. The new focal plane instrumentation to be outfitted on SOFIA is expected to have ten times the point source sensitivity and three times the angular resolution of its predecessor. Scientists believe SOFIA will be capable of studying the entire lifecycle of the stars and planets by examining infrared emissions of different phases of the interstellar medium.

Davis' principal contribution to KAO research has been in the development and use of a cryogenically-cooled infrared multiplexing Fourier transform spectrometer. The spectrometers that are to fly aboard SOFIA will need to take advantage of its augmented sensitivity to increase their spectral resolving powers where needed.

Further developments in spectrometer design will be used on SOFIA, including an innovative optical multiplexing technique for infrared imaging being pursued by Davis [Ref. 2]. This technique is based on the use of orthogonal function encoding of entire images at once, rather than on traditional raster scanning methods.

Davis [Ref. 2] proposes that a unique state-of-the-art imaging/spectroscopic system can be developed that will take advantage of Fourier spectroscopic methods to image in both the spatial and spectral domains simultaneously. Davis believes extreme sensitivity and versatility can be achieved on a platform such as SOFIA. If successful, the imaging spectroscopic system could also significantly impact such areas of infrared remote sensing as passive surveillance and target signature identification.

B. THESIS GOAL

The goal of this thesis is to provide the initial design and testing of a precision, closed-loop, servo drive system that will, eventually, rotate and position the orthogonal function encoding masks in Davis' imaging/spectroscopic system. This effort was basically proof-of-concept in nature. The shaft position encoder mechanism used in this particular study was an inexpensive digital opto-mechanical encoder, known from the start of the project to lack the resolution necessary for use in the eventual prototype instrument. The next generation position encoder will be a high resolution phase-locked loop analog encoder. This new encoder will comprise the work of a future thesis study. Thus, the project did not set out to achieve extremely sensitive positioning standards, but rather to establish a performance baseline to which a more precise position

encoding system could be retrofitted and refined. This effort will lay the groundwork for future experimentation leading to the development of high speed and resolution infrared spectroscopic imaging instruments using this servo drive system to its fullest potential.

II. NATURE OF THE EXPERIMENT

A. SYSTEM OVERVIEW

This thesis involved the design and prototyping of a closed-loop (feedback) motor servo drive system in support of the development of a new initiative in the field of infrared remote sensing. Davis [Ref 2] proposes to use a rotating disk to contain the imaging encoding masks in his new instrument, a sketch of which is provided in Figure 1. To maximize the data acquisition rate, a motor servo must rotate an ensemble of masks into the image path and position the mask rapidly, with a high degree of accuracy.

The proposed motor servo drive system is comprised of a high torque, direct current motor mechanically attached to a shaft angular position encoder. The signals from the shaft encoder are fed through an electronic feedback circuit to produce an amplified, negative feedback signal. The circuit is designed to have the capability for an analog voltage positional signal to be added to the feedback signal, thereby altering the steady-state operating point of the closed-loop system and, hence, the motor's preferred lock-on position.

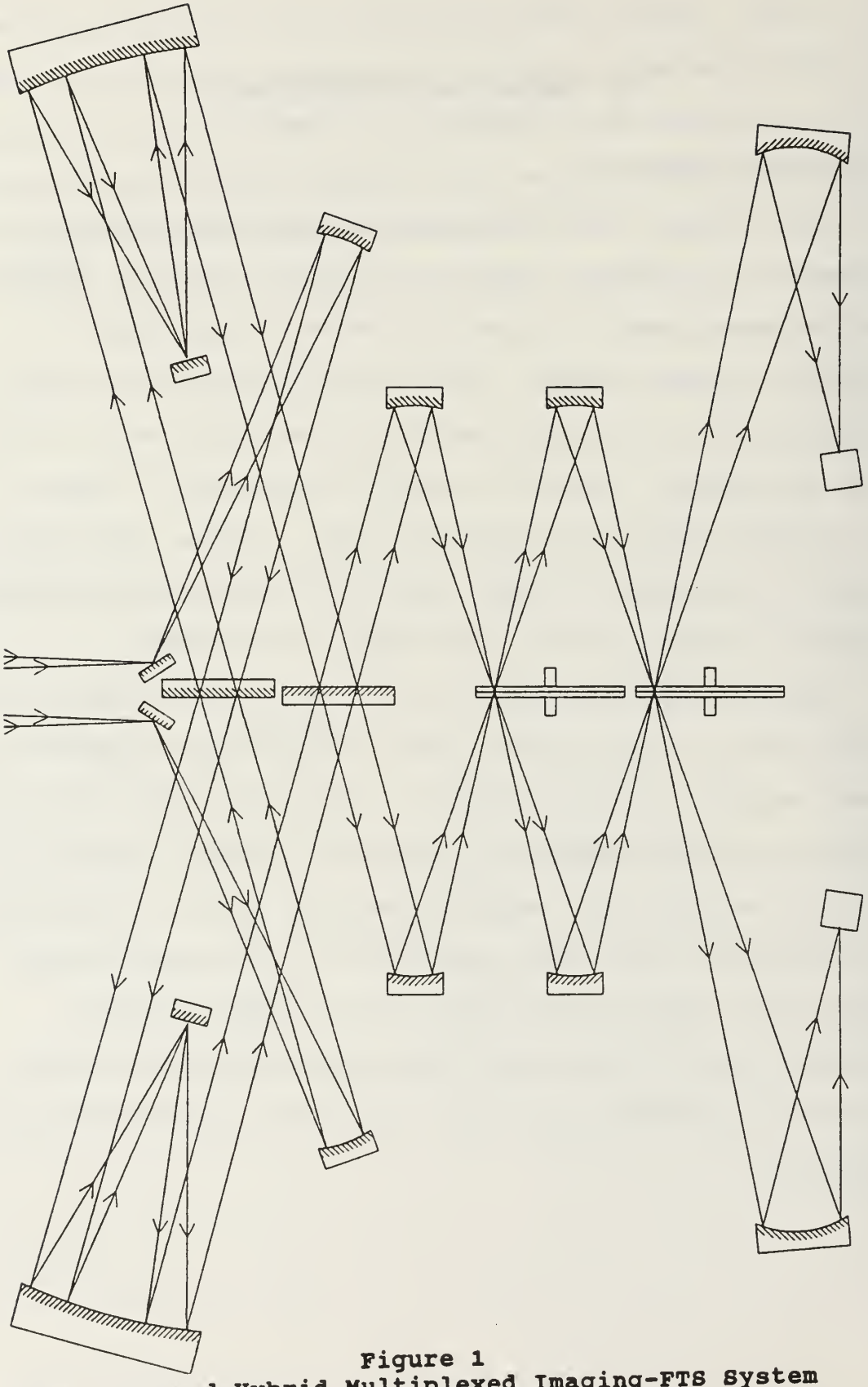

Figure 1
The Proposed Hybrid Multiplexed Imaging-FTS System

The servo drive motor is powered by a high power operational amplifier in order to achieve extremely stable, fast and accurate response to an input position signal.

B. SERVO DRIVE REQUIREMENTS

An optimal servo drive must satisfy several performance criteria, some of which are mutually contradictory. This state of affairs forces compromises in the engineering design. Below are listed general considerations in the design of a servo drive system.

1. Frequency Bandwidth

A powerful electric motor is a substantial inductive load. The response of an inductive load at different frequencies changes as a result of phase shifts between the input voltage to the voltage across the inductive load. The feedback system must be designed with this in mind. The most difficult perturbation to a servo system would be its response to an abrupt change in its input voltage, such as a square wave. A square wave contains an infinite number of harmonic frequencies to which the servo system must respond accordingly. The ideal response to a square wave input would be, of course, an instantaneous motion of the motor that would track the square wave exactly.

2. Torque Considerations

In order to accelerate the inertial load attached to the motor shaft, including both the external mechanical load

and the motor's intrinsic moving parts, the motor must be able to produce substantial torque. Torque is produced in a direct current motor by a current passing through a series of coil wires in a strong magnetic field. A forceful motor response is very important when changing the angular velocity of the motor, for example, accelerating from a stop, or reversing direction while rotating.

3. Friction

The servo motor must be relatively free of friction to ensure maximum speed can be attained in with minimal torque by the motor. Minimal friction ensures that the torque required for system response over a broad band of frequencies is directly proportional to motor current. This results in a simple linear system that is capable of responding to a wide variety of inputs, including the square wave mentioned above.

4. Accuracy

To be useful in accurately positioning the motor shaft to a desired angular location, the servo drive feedback system must have sufficient gain to move the attached load in response to the slightest feedback signal, even in the presence of some inevitable friction.

5. Stability

The system must be stable at the heightened gain condition required for accurate control, that is, not be

subjected to high frequency oscillations while continuously seeking to lock on to the preferred position. Stability is also affected by the high frequency phase shift produced by the inductance of the motor coils. It is possible to have a condition in which the input stimulus is 180° out of phase with the motor coil voltage, causing an unstable, runaway motor response rather than the desired tracking of the input signal.

III. EXPERIMENTAL PROCEDURE

A. GENERAL APPROACH

The general approach taken on developing a servo system satisfying the aforementioned performance criteria was broken down into five phases. The first phase of the development was a mathematical modeling of a DC motor system to a given input stimulus. The next phase involved the circuit parts selection and design. The third phase was the development of individual electronic subsystems within the servo system on a prototyping breadboard. The forth phase was the fabrication of a hard-wired version of the electronics mounted on a sturdy platform. The fifth and final phase was the testing and performance evaluation of the finished system.

The following sections of this chapter detail the methodology of the effort involved in each phase.

B. MATHEMATICAL MODELING OF SYSTEM PERFORMANCE

1. Background

a. Feedback System Analysis

A servo system is basically a closed-loop, negative feedback system that uses, at the very least, both electronics and electromechanical components in portions of the closed feedback loop. Before getting into specifics

regarding the composition of the servo system, a general description of the components which comprise a generic closed-loop (feedback) control system would be useful.

According to DiStefano, Stubberud, and Williams [Ref. 1:p. 3], a closed-loop control system is one in which "the control action is somehow dependent on the output." They also define feedback as the characteristic of a closed loop system which enables the system output to be compared with the input so that the necessary control action may be constructed as a function of the output and input. The following figure is a block diagram of a feedback control system adapted from DiStefano, Stubberud, and Williams [Ref 3:p. 13].

The following definitions, also adapted from DiStefano, Stubberud, and Williams [Ref 3], apply to the components of the block diagram:

- The plant, also known as the controlled system, is the item or process that is to be controlled.
- The control elements, also known as the controller, are the components which generate the appropriate control signal to the drive the plant.

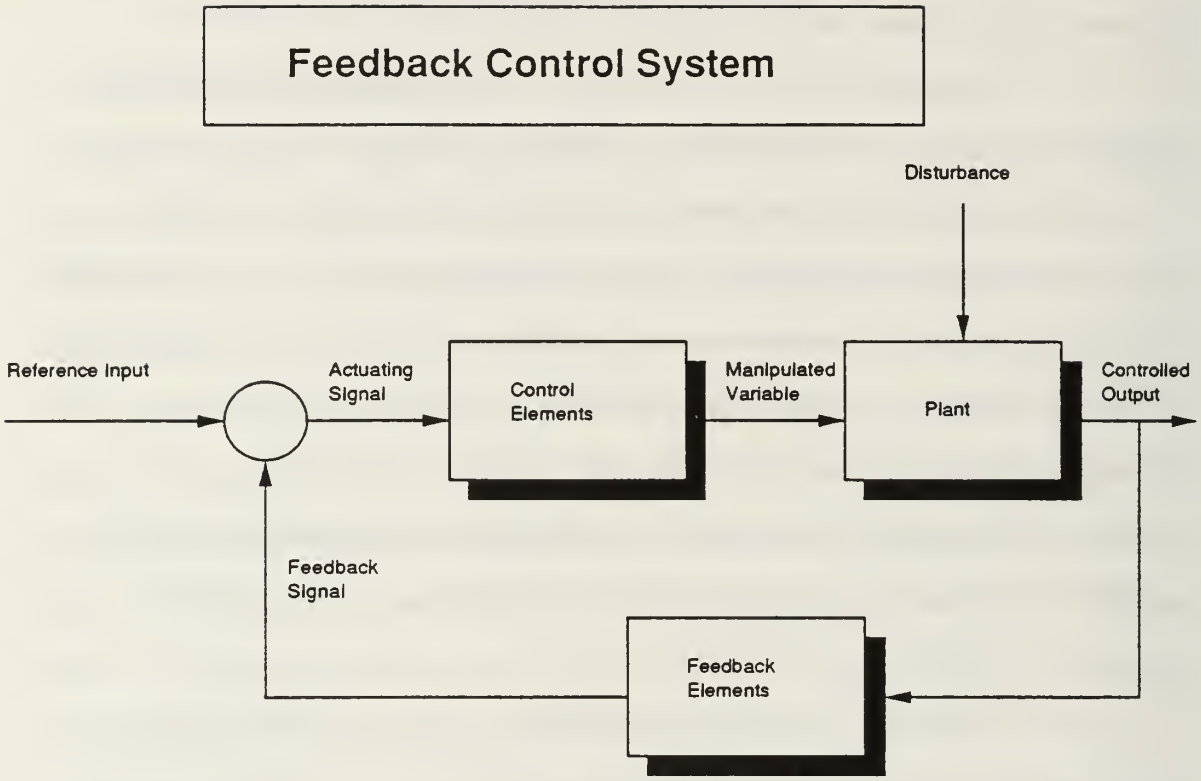

Figure 2
Feedback Control System Block Diagram

- The feedback elements are the components required to form the functional relationship between the feedback signal and the controlled output.
- The reference input is the external signal applied to the feedback control system to execute a specified action of the plant.
- The plant generates an output that is controlled.
- The feedback signal, also known as the loop error signal, is the signal which is a function of the controlled output. The feedback signal is algebraically summed with the reference input to obtain the actuating signal.
- The control signal is the quantity or condition which the control elements apply to the plant.
- A disturbance is the undesired influence or perturbation signal which affects the value of the controlled output.

The terms defined above can be related to the servo system designed in this thesis. The plant to be controlled is the angular position of a motor shaft. The control signal is the current produced by a high power operational amplifier. The feedback elements are a shaft position encoder, an encoder analog conversion circuit, and a preamplifier circuit. The reference input will, in future upgrades to the servo system, be generated by computer though the use of a digital-to-analog conversion board. For

prototyping purposes, a signal generator provided the reference input. The controlled output is the DC motor shaft position. The disturbance is any undesirable external perturbation that would cause the shaft angular position to deviate from the nominal, desired configuration. The relationships to the other defined terms above are obvious.

b. Brief Review of Direct Current Motor Theory

A direct current motor is described by Kuo [Ref. 4:p. 167] as a "torque transducer that converts electrical energy into mechanical energy." The torque is produced by the interaction between a uniform, radially oriented magnetic field generated by a collection of permanent magnets and the current traveling in the armature coil wire.

Kuo [Ref. 4:p. 172] states that it can be assumed in modeling a DC motor that the torque developed by the motor is proportional to the magnet-armature air gap magnetic flux and armature current. In order to achieve a large torque from the motor system, substantial current must be maintained on the motor.

c. Electrical Analysis of Motor Circuit

The electric current flowing through the motor circuit is subjected to an impedance comprised of both resistive and inductive terms. In addition, the rotation of the armature coil through the magnetic field of the permanent magnets generates a "back" electromotive force

(emf). The equivalent electric circuit can be modeled as shown in Figure 3.

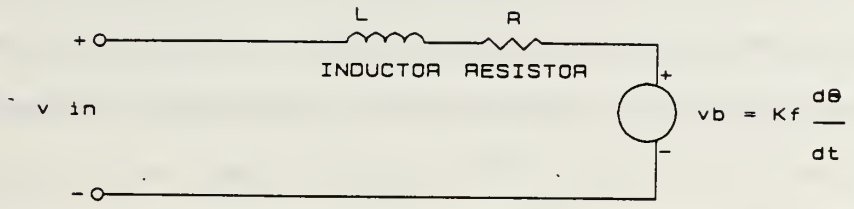

Figure 3
Electrical circuit model of DC motor

d. Mechanical Influences on System Performance

There are many similarities between the electrical and mechanical impedances in the motor circuit. Whereas the product of a resistive constant (resistance) and electron flux (current) results in a force (voltage) in the electrical sense, the product of a friction constant and shaft velocity on moving parts of the motor system causes a force in the mechanical sense.

In addition, much like the reactive load in the motor windings discussed above, the performance of the servo drive system is influenced by inertial loads from rotating masses internal and external to the electric motor.

2. Solution of Differential Equation

Both electrical and mechanical components of the influences on the performance on a DC motor can be combined in a single differential equation describing the system reaction to a given force (voltage). The mathematical model employed in deriving the theoretical performance in the servo drive system was adapted from DiStefano, Stubberud, and Williams [Ref. 3: p. 107] and Kuo [Ref. 4: p. 171]. The following definitions will be used throughout this analysis:

i - Electrical current through the motor circuit.

L - Motor inductance

R - Motor winding electrical resistance

K_f - Proportionality constant applied to shaft rotational velocity to derive back emf voltage.

K_t - Proportionality constant applied to current in motor windings to derive torque output of motor.

v_b - Back EMF resulting from the rotating armature Equivalent to $K_f d\theta/dt$.

θ - angular position of the motor shaft.

T - torque generated by motor.

B - total viscous friction from all moving parts.

J - Total inertial load (motor and load).

v_i - voltage impressed on motor.

It is significant to note that Kuo includes an additional term $T_L(t)$ in his development of the differential equations. According to Kuo, $T_L(t)$ represents the torque that the motor has to overcome in order to have motion,

i.e., as a result of static friction. This term creates a great difficulty in formulating a solvable differential equation, as it cannot be considered as a linear term. Kuo states that it is set to zero after presenting the same Laplace transform of the time dependent form of the differential equation that is offered below. The term is therefore also left out of the mathematical model in this thesis.

With the above considerations in mind, the differential equations of the motor armature circuit and the inertial load are

Motor Armature

$$Ri + L\frac{di}{dt} = v_i - K_f\frac{d\theta}{dt} \quad \text{and} \quad \text{Inertial Load} \quad K_t i = J\frac{d^2\theta}{dt^2} + B\frac{d\theta}{dt}. \qquad (1)$$

The Laplace transform of the two equations in (1), with initial conditions zero, is

$$(R + sL)I = V - K_f s\theta \quad \text{and} \quad K_t i = (Js^2 + Bs)\theta. \qquad (2)$$

A simultaneous solution of the equations in (2) to establish a transfer function between V and θ is

$$\frac{\theta(s)}{V(s)} = \frac{K_t}{(Js^2 + Bs)(Ls+R) + K_t K_f s}. \qquad (3)$$

After rearranging terms in equation (3), an alternate form of the transfer function is

$$\frac{\theta(s)}{V(s)} = \frac{K_t/JL}{s[s^2 + (B/J + R/L)s + ((BR+K_tK_f)/JL)]} . \quad (4)$$

The next step in solving the differential equation entails breaking the quadratic term in the denominator into the product of two expressions. Without going through the algebraic manipulations, the quadratic term can be replaced with

$$\left[s + \frac{BL+RJ+X^{1/2}}{2JL} \right] \left[s + \frac{BL+RJ-X^{1/2}}{2JL} \right] , \quad (5)$$

where $X = [(BL-RJ)^2 - 4JLK_tK_f]$.

At this point, the transfer function is in a form that can be solved using usual inverse Laplace transformation methods. To reduce confusion in the solution of the equation, the following substitutions will be made.

$$\text{Let } A = \frac{BL + RJ}{2JL} \quad \text{and} \quad C = \frac{[(BL-RJ)^2 - 4JLK_tK_f]^{1/2}}{2JL} . \quad (6)$$

Equation (4) can therefore be represented in the following form,

$$\theta(s) = \frac{K_t\ V(s)}{JL} \left[\frac{1}{s(s+A+C)(s+A-C)} \right] . \quad (7)$$

Employing the method of partial fraction decomposition, equation (7) can be expanded to

$$\theta(s) = \frac{K_t\ V(s)}{JL}\left[\ \frac{x}{s}\ \frac{y}{(s+A+C)}\ \frac{z}{(s+A-C)}\ \right] \quad . \tag{8}$$

The method to determine x, y, and z is tedious but algebraically straightforward. The solutions are

$$x = \frac{1}{(A^2\ -\ C^2)}\ , \quad y = \frac{1}{2C(A+C)}\ , \quad z = \frac{1}{2C(C-A)}\ . \tag{9}$$

Combining equations (8) and (9), the transfer function is presented in a form capable of being converted back to the time domain. The relationship between θ and V is

$$\theta(s) = \left[\frac{K_t}{JL(A^2-C^2)}\right]\frac{V(s)}{s} + \left[\frac{K_t}{2JLC(A+C)}\right]\frac{V(s)}{(s+A+C)} + \left[\frac{K_t}{2JLC(C-A)}\right]\frac{V(s)}{(s+A-C)}\ . \tag{10}$$

Inverse Laplace transformation of equation (10) to the time domain is

$$\theta(t) = \left[\frac{K_t}{JL(A^2-C^2)}\right]\int_0^t V(\tau)\,d\tau + \left[\frac{K_t}{2JLC(A+C)}\right]\left[V(t) * e^{-(A+C)t}\right] - \left[\frac{K_t}{2JLC(A-C)}\right]\left[V(t) * e^{-(A-C)t}\right]\ . \tag{11}$$

Variables A and C are as defined in equation (6). The system response is thus found to be the sum of three terms. One term involves an integral over the time in which the voltage is applied to the motor, while the other two are the convolution of the voltage applied to the motor and an exponential term describing the response of the system. The numerical solutions of the equation given various stimuli required the use of the commercial equation-solving program called MathCAD.

Equation (11) was entered into MathCAD version 2.0 using hypothetical values close to those measured for the actual motor used in this thesis. The results of MathCAD can be found in Appendix A. The predefined units documented at the last page of the MathCAD calculation were tracked by MathCAD throughout the calculation to ensure the correctness of the equations.

The convolution of the applied voltage with the system response terms was the difficult part to the MathCAD setup. However, noting that the convolution of two terms in the time domain is equivalent to the multiplication of their Fourier transforms made the time domain solution of the equation relatively simple. The Fourier transform of the terms were calculated and multiplied by MathCAD. The inverse Fourier transform was then taken of the product.

The initial results obtained from this process did not, however, turn out to be accurate. MathCAD apparently

applies a multiplication factor equal to the reciprocal square root of the number of samples taken in the Fourier transform. It apparently multiplies the inverse Fourier transform by an identical factor. In the convolution calculation, however, two frequency domain quantities are multiplied and then their product is inverse transformed back to the time domain. The net effect was that the MathCAD output was improperly scaled by the factor described above. This improper scaling is evident in the final MathCAD calculation of the second and third terms of equation (11).

The graph provided on the second page of the MathCAD printout shows the motor response (no feedback) to a voltage pulse of arbitrary length. The quadratic shape of the response curve while the voltage is applied is typical for the acceleration of the motor. The ringing in the output is apparently the result of the motor internal inductance reacting with the self-inductance back emf term, v_b.

C. SYSTEM DESIGN

1. Motor Selection

A Clifton Precision Model DH-3250-C-1, high torque permanent magnet servo motor was selected from the Herbach & Rademan Company in Philadelphia, Pennsylvania. The motor was chosen because it would run on 12 volts direct current, had dual shafts, was easily mountable, and could be run at

12 amperes maximum current. The only documentation available for the Clifton Precision servo motor was the catalog specification. A copy of the catalog specification is provided in Appendix B.

2. Power Operational Amplifier Selection

A National Semiconductor Model LM12 150 Watt operational amplifier was chosen to power the servo motor. The operational amplifier was chosen because it could deliver 10 amperes (bipolar) from a wide range of supply voltages. A specification sheet of the LM12 operational amplifier can be found in Appendix C.

3. Power Supplies

Two Power-One Model HD24-4.8-A 24 volt DC power supplies were chosen to drive the entire system. The power supplies could each deliver 4.8 amperes of current, and were available from the National Stock System. A specification sheet for the Power-One 24 volt power supplies can be found in Appendix D.

4. Cage Design

A sturdy metal cage was needed to house the motor and to provide the means to mount a shaft position encoder without allowing any mechanical flexure between the motor and encoder. The cage design was set forth on the drawing found in Appendix E. The material for the cage was

standard shelving, heavy-gauge angle sheet steel with bolt holes prepunched for easily assembly.

5. Shaft Position Encoder

A Clarostat Model 601V opto-mechanical shaft encoder was chosen because it provided an inexpensive means to begin the design of the servo subassembly. It requires only 5 volts DC, and provides TTL logic output in quadrature (90° ± 45°), as shown in Figure 4, at a rate of 128 pulses per channel per revolution. The only information available for the Clarostat shaft encoder is the catalog specification. A copy of the catalog specification for the shaft encoder is found in Appendix F.

6. Motor - Encoder Coupling

A custom coupling was designed to connect the 0.5 inch diameter shaft of the motor to the 0.25 inch shaft of the encoder. The coupling material was chosen to be aluminum to minimize inertial effects while to maximize torsional strength. Small set screws were installed on each opening in the coupling to lock the shafts into position. An engineering design drawing of the coupling is found in Appendix G.

7. Encoder Analog Conversion Board

A circuit was designed to take the encoder digital signals and to convert them to an analog voltage which varied linearly with shaft angular position. The final

circuit schematic is found in Appendix H. Low-power Schottky TTL logic integrated circuit chips were used in the design.

Square wave TTL pulses are sent from the encoder in quadrature, which means that depending on the direction of the rotation of the encoder shaft, the pulses on the encoder channel A or B lead or lag each other by approximately 90°. The pulses on encoder channel A (pin 2) are fed to the clock input on the first 74LS74 edge-triggered, D-type flip-flop (U1A), the D input on the second edge-triggered, D-type flip-flop (U1B), and also to a standard 74LS00 NAND gate (U2A). Copies of the manufacturer's data sheets for the 74LS74 flip-flop and the 74LS00 NAND gate are provided in Appendices I and J.

In the same manner, the pulses on encoder channel B (pin 4) are fed to the clock input on the second edge-triggered D-type flip-flop (U1B), the D input on the first edge-triggered D-type flip-flop (U1A), and also to a standard NAND gate (U2D).

The operation of the flip-flop/NAND gate combination is straightforward. When the encoder is rotating in the "forward" direction, the pulses from channel A lead the pulses from channel B by approximately 90°. This causes flip-flop U1A to latch a TTL "high" signal on the Q output. This high signal causes the NAND gate to allow the negation

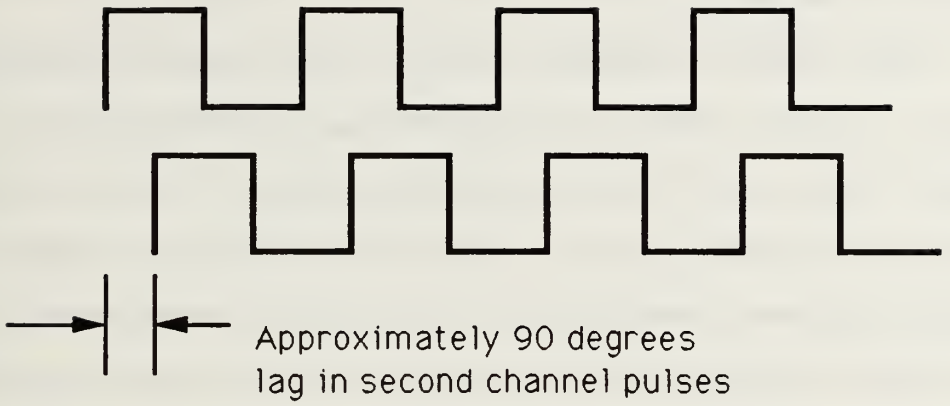

Figure 4
Typical dual channel encoder signals in quadrature.

of the pulse train from encoder pin A to pass on to the up-down counter, U3. As the pulse train from pin B of the encoder fed to U1B clock input lags the pulse train from pin A of the encoder fed to the D input, flip-flop U1B remains off, with a TTL "low" signal on the Q output. With one input to the NAND gate always low, the output of the NAND gate is always high (when the encoder is rotated in the forward direction). The 74LS193 up/down counter requires this high signal on the inactive up or down input in order to count the active pulsing input. A copy of the

manufacturer's data sheet for the 74LS193 up/down counter is provided in Appendix K.

Each up/down counter can maintain 4 binary signal outputs. As the first counter exceeds its count at 15, it passes a carry output to the second counter. In all, the two counters can support a total count of 256 (0 - 255). The 74193 up/down counters are fully programmable, that is it has the capability of being preset to a certain level on any of the 4 outputs by entering that level on the data input (A,B,C,D) while the load input is low. That capability was utilized in this design with 5VDC applied to the 2.2K ohm resistor connected to pin 9 of the second up/down counter, U4. Thus when switch SW2 is closed, the overall count is programmed, or preset, to 128. The intent of this feature is to preset the nominal servo position, corresponding to 128, so that the shaft position could then be monitored for a full turn (128 pulses) in either rotation direction.

The 256 binary counts are fed to an 8-bit digital-to-analog converter (DAC), U5. The DAC connections conformed to recommendations in the typical application on the DAC0808 National Semiconductor data sheet. The data sheet is provided in Appendix L. The output of the conversion board is a negative current that provides the necessary signal input to the first stage of the amplifier board.

Two microswitches were designed into the circuit for calibration purposes. The first switch, SW1, sets the position count to zero. The second switch, SW2, sets the position count to 128, corresponding to the nominal operating position. The intent of switch SW1 was to allow a count reset in which the minimal voltage could be established easily during the development of the system. It serves no formal purpose in the finished product. Switch SW2 is more important in that system setup and calibration require the nominal position to correspond to the preferred "zero" shaft position. With the motor turned off (switch SW3), the null offsets (R10 and R15) can be fine tuned. After this initial set up, no additional tuning is necessary.

8. Amplifier Board

A series of operational amplifiers boost the voltage of the position signal to provide the necessary negative feedback to the motor to servo it into position. The total signal from the encoder circuit is input to the amplifier circuit having a voltage range of approximately -10 to 0 volts DC (measured across the 2.2K ohm resistor R12 on the feedback amplifier circuit schematic (Appendix M), depending on the shaft position. A null offset is applied at the input so that the input signal reads zero volts at the nominal shaft position. This signal varies up or down on

either side of zero volts as the shaft rotates clockwise or counterclockwise.

Two LM324 quad operational amplifier ICs were used in the final design of the amplifier circuit for simplicity and board space limitation reasons. A copy of a representative manufacturer's data sheet is provided in Appendix N.

The values of the feedback resistors which determine the amount of gain from each amplifier were chosen fairly arbitrary; however, a few constraints had to be considered. First, the input resistor to each amplifier stage had to be fairly small, in the 1000 ohm range, so as to be much less than the input impedance of the operational amplifier. Secondly, the gain of each amplifier stage had to be fairly small, on the order of 20 or 30, so that the null offset of the encoder "zero" position could easily be adjusted. In addition, with smaller increments of gain in each amplifier stage, the overall circuit performance seemed to be more stable than with a single large gain amplifier. Fine adjustments to the circuit's overall feedback gain were possible using standard grade potentiometers. Lastly, with several amplifier stages, convenient voltage summing points were available in the circuit during the prototype development.

The signal is boosted to the level in which a shaft rotation from the nominal position of ±1 count on the

encoder circuit causes (approximately) a ±5 volt signal to be applied to the motor power amplifier. Likewise, a shaft rotation of ±2 counts in either direction results in a ±10 volt signal at the input to the motor power amplifier. The signal is designed to saturate for three counts in either direction at approximately ±15 volts. A "potential well" is therefore created that maintains a stable preferred position. The selection of the voltage levels mentioned above was a significant portion of the system development and is discussed in greater detail in the System Testing chapter.

A separate set of operational amplifiers serve as a high-pass Butterworth-type filter to boost the higher frequencies of the incoming position feedback signal to enhance the servo system's response at higher frequencies. Further discussion of the high frequency requirements for this system can be found in the System Testing chapter.

9. Motor Driver Power Operational Amplifier

The amplified encoder feedback signal is sent to the National Semiconductor LM12 150 Watt power operational amplifier circuit. The schematic of the motor power amplifier circuit is provided in Appendix O. The LM12 was selected because of several desirable features. According to its catalog specification sheet, provided in Appendix C, the LM12 is capable of delivering ±10 amps output current at

any output voltage, while being completely protected against overloads, including short circuits to the power supplies. These features made the LM12 ideally suited to the expected demands of a high torque servo motor.

Although the LM12 has internal overheating protection, a heat sink was selected so that the power amp could operated continuously high load with minimal degradation in performance due to internal heat generation. A large, extruded aluminum, black anodized heat sink designed for a 3 pin TO-3 integrated circuit package was modified to allow sufficient clearance for the unusual 4 pin configuration of the LM12.

The basic design of the LM12 circuit is that of a voltage follower. According to Rutkowski [Ref 5, p. 54], an operational amplifier configured as a voltage follower provides the circuit both an extremely large input resistance while being fully capable of driving a low resistance load.

The catalog specification sheet for the LM12 recommended that the voltage supply leads to the operational amplifier be by-passed with low-inductance capacitors having short leads and located close to the LM12 package terminals to avoid spurious oscillation problems. The catalog specification claimed that the LM12 is stable with "good-quality" electrolytic bypass capacitors greater than

20 μF. A convenient value of 47 μF was selected for this application.

Due to the highly inductive load that the servo motor places on the LM12, output clamp diodes were installed between the LM12 output and the voltage supplies to the LM12. According to the LM12 catalog specification, the stored energy in the load inductance can drive the output voltage outside the supply voltages. The specification states that, although the LM12 has internal clamp diodes, extreme conditions can cause destruction of the IC. The specification explains that National Semiconductor's experience with the LM12 is that random failures will occur if the output to the LM12 is hard-wire shorted when external clamp diodes are not used and the supply voltages are above ±20 volts. As the LM12 is intended to be operated at voltages of ±24 VDC, the clamp diodes are very necessary. Large diodes of type IN5408 were chosen for this purpose.

In the voltage follower configuration used in this thesis project, the op amp is highly susceptible to low amplitude oscillation. The oscillation, according to Horowitz and Hill [Ref. 7, p. 245], occurs when the open-loop phase shift reaches 180° at some frequency at which the gain is greater than one. At that frequency, negative feedback becomes positive feedback. This situation provides the necessary condition for oscillation.

To reduce the possibility of oscillation in an uncompensated op amp such as the LM12, the manufacturer and Horowitz and Hill [Ref. 7, p. 245] recommend unity-gain frequency compensation. By utilizing the R-C combination proposed by the manufacturer to reduce feedback at higher frequencies, the LM12 was stabilized.

Further discussion regarding feedback oscillation in the LM12 can be found in the electronics prototyping subsection under the System Assembly section.

All wiring to the motor that would be expected to carry loads over 1 amp was at least 14 gauge in thickness to minimize voltage losses due to wire resistance.

10. Voltage Regulator Circuit

A final addition was made to the amplifier circuit described above in order to provide for conversion of the ±24 VDC input voltage to the +5 VDC and ±15 VDC needed by the operational amplifiers, and encoder DAC circuit and the encoder itself. Three IC chips were selected to perform this task. The LM7805, LM7815, and LM7915 chips were chosen because of their availability. Capacitors were placed on the output of each convertor to ensure a filtered voltage output, as was recommended by the individual manufacturers' data sheets.

Copies of the LM7800 and LM7900 series voltage regulator data sheets are provided in Appendices P and Q.

D. SYSTEM ASSEMBLY

1. Motor - Encoder Cage Assembly

A sturdy metal cage was assembled following the design in Appendix E, using heavy duty shelving braces. The angular braces were bolted together using one inch long, 5/16" course-threaded bolts with lock washers and nuts. Two strong bars were mounted horizontally on the front of the cage spaced at a distance sufficient for the motor shaft clearance. Two brackets were installed within the cage approximately 6 inches from the front of the cage to provide locations to bolt the encoder mounting bar.

The finished cage assembly was mounted to a one inch thick piece of plywood to provide additional vibration resistance.

A photograph of the completed cage - plywood base assembly is provided in Figure 5.

2. Motor - Encoder Mounting

The next step in the assembly process was to mount the DC motor and shaft position encoder in the cage. Four holes were drilled in the 1 1/2" wide mounting bars on the front of the cage in locations corresponding the hole pattern on the front of the motor. Four 1/2" long 8/32 stainless screws were installed to secure the motor to the mounting bars. The mount was considered sufficiently sturdy that rear mounting bars were not used.

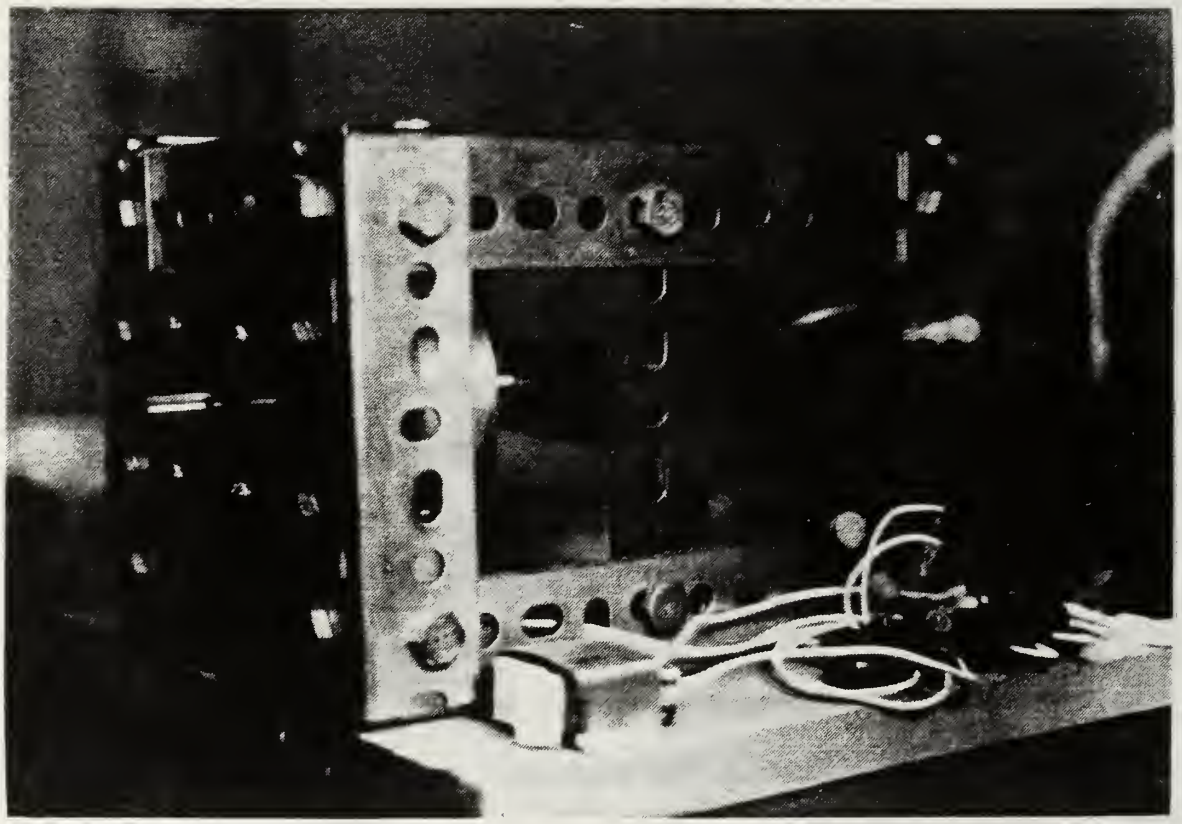

Figure 5
Photograph of Cage Assembly and Plywood Base

An aluminum motor-encoder coupling was mounted onto the rear 1/2" diameter shaft. A photograph of the finished coupling is provided in Figure 6. The coupling was secured to the motor shaft using a 6/32 set screw. A 9/16" hole was drilled in a 6" long, 1 1/2" wide horizontal bar to accommodate the encoder mounting shaft. Two 3/8" holes were drilled at opposite ends of the bar to mount to the brackets within the cage.

A simple procedure was followed to avoid preloading stresses on the encoder shaft. During early tests the preloading stresses were found to cause a great deal of rotational friction. The encoder was loosely inserted into the motor-encoder coupling and all mounting bar bolts were first tightened. Next, the encoder shaft nut was tightened. Finally, before tightening the encoder shaft set screw, the coupling alignment was rechecked by rotating the motor shaft while ensuring that the encoder shaft did not rotate.

A photograph of the motor and encoder mounted in the cage is provided in Figure 7.

3. Assembly of Power Operational Amplifier.

After modifying the aluminum heat sink mounting hole pattern to accommodate a 4 pin TO-3 IC package, the LM12 power amplifier was installed in the aluminum heat sink using two 3/8" long 6/32 screws. A thermally conductive

Figure 6
Motor-Encoder Shaft Coupling Photograph

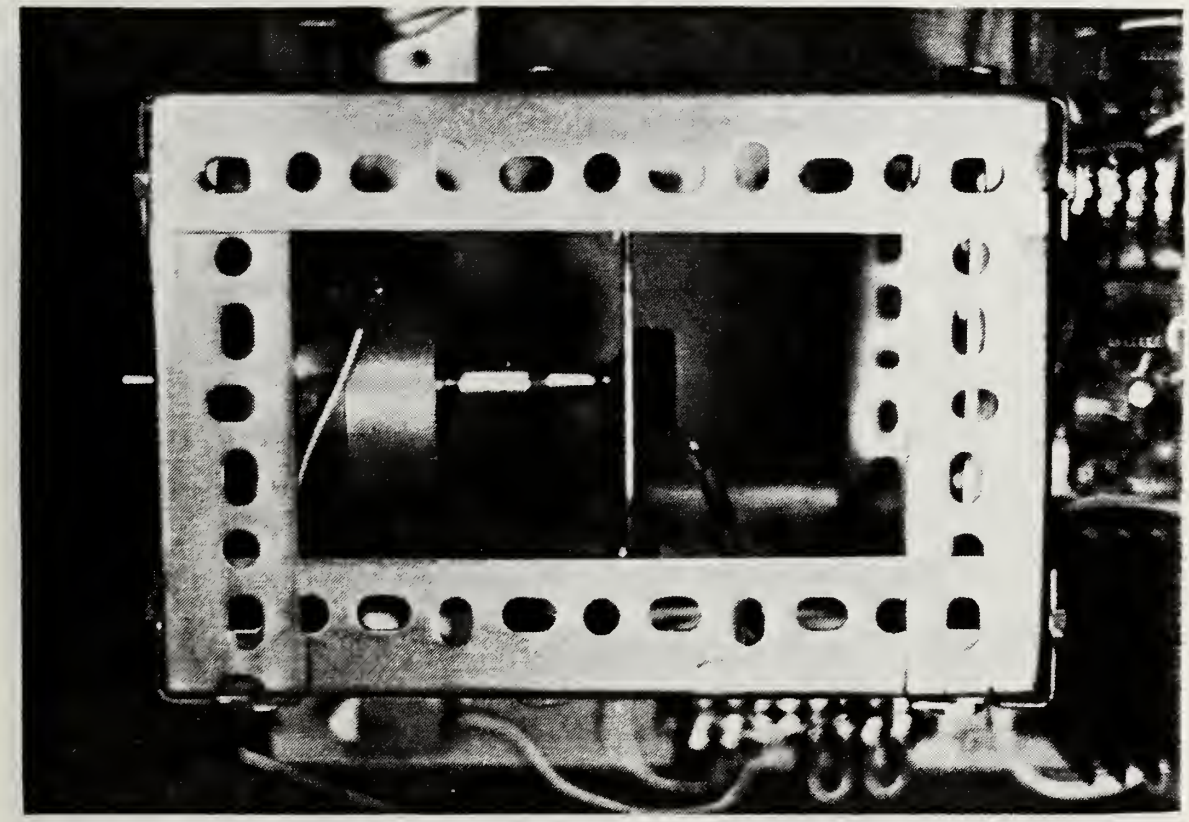

Figure 7
Photograph of Motor and Encoder Mounted in Cage

heat sink compound was used to ensure good thermal contact between the IC package and the heat sink.

It is important to note that the case of the LM12 is the negative voltage supply input. The heat sink is, in all likelihood, at a potential of -24 VDC when the system is powered up. This was not a problem during the prototype testing because the heat sink was mounted to a plywood base. If it is to be in electrical contact with ground or any other component in a future design, a thermally conductive, electrically insulating washer such as mica or anodized aluminum should be installed between the IC and the heat sink and some thermal compound should be placed on both faces of the washer.

A photograph of the LM12 power operational amplifier mounted on the heat sink is provided in Figure 8.

4. Electronics Prototyping

a. Encoder Analog Conversion Circuit

The encoder analog conversion circuit was first assembled on a Global Specialties Protoboard Model PB-503. A photograph of the protoboard is provided in Figure 9. The protoboard was ideal as it provided the +5VDC, ±15VDC and a common ground point needed for the ICs and encoder described in the System Design section C.7. The protoboard also provided an excellent reference signal in the form of either a square, triangle or sinusoidal waveform.

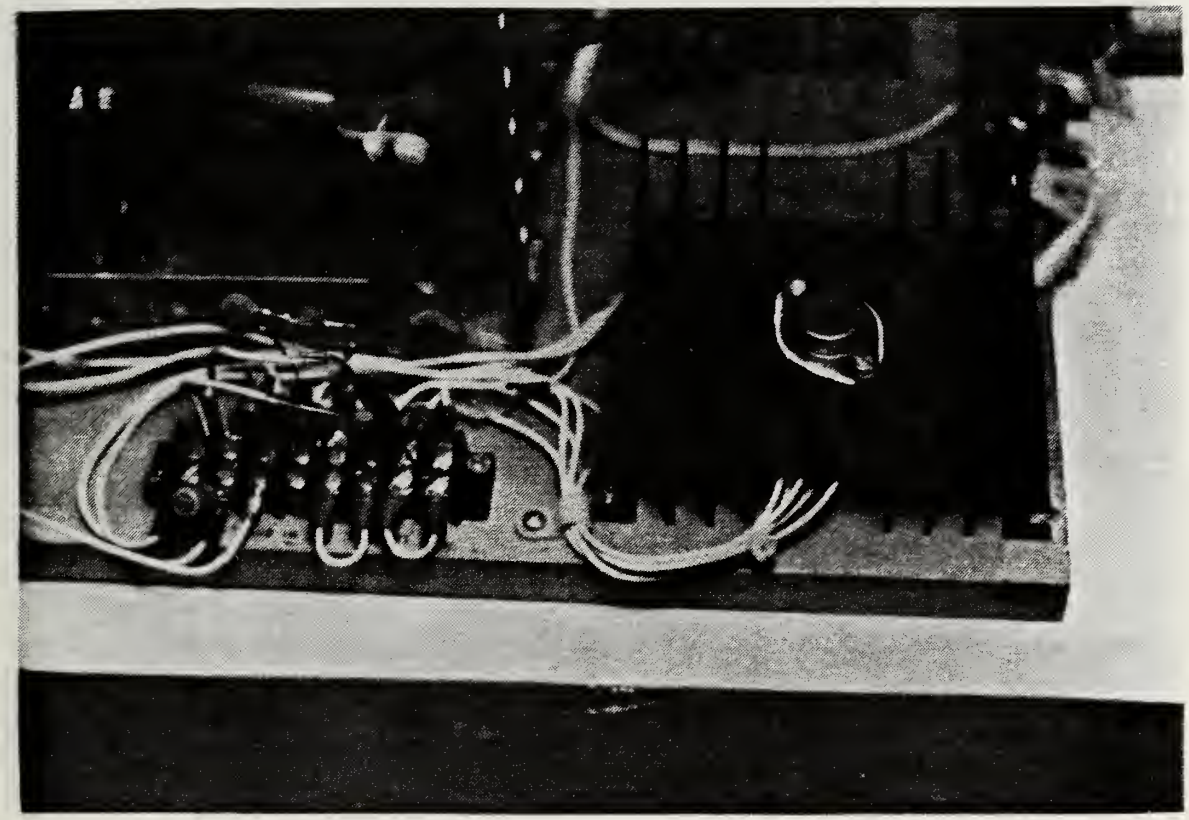

Figure 8
Photograph of LM12 Op Amp and Heat Sink Assembly

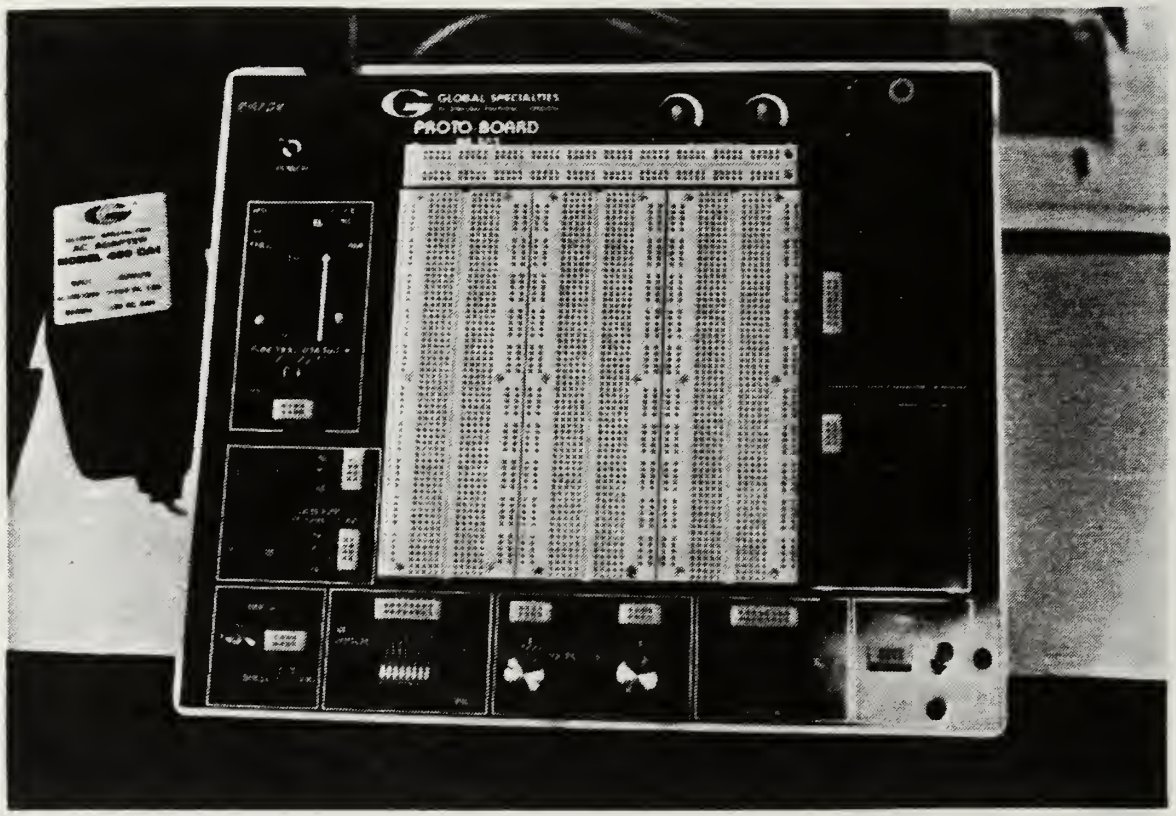

Figure 9
Global Specialties Protoboard Model PB-503

The prototyping of the encoder analog converter was very successful in that the early design produced a uniform, linear, digital-to-analog converter output as was needed.

One point worthy of note concerns the DAC positive reference current, I_{14}. According to the manufacturer's data sheets for the DAC0808 Digital-to-Analog converter, the maximum current to be applied on pin 14 is 5 mA. Unpredictable output from the DAC resulted from accidently exceeding the I_{14} current limit during prototype testing. Care must be taken in ensuring the resistor value between pin 14 of the DAC and +15 VDC is greater than 3000 ohms. A resistance of 6.2K ohms was determined to provide satisfactory stability over the full range of voltage output by the DAC.

b. Feedback Amplifier Circuit

After the prototype encoder circuit was transferred to a hardwired circuit card, an amplifier circuit was prototyped on the same protoboard mentioned above. The amplifier circuit initially employed several LM301 high gain operational amplifiers. They were used because of their easy availability and simple design. A copy of the LM301 manufacturer's data sheet is provided in Appendix R.

The prototyping of the amplifier circuit was very difficult because of the author's lack of familiarity with

the operation of the LM301 op amps. Several unsuccessful designs were attempted. After many instructional meetings with the thesis advisor, a successful combination of inverting operational amplifiers tied together in series was found experimentally to address these problems. An approximate total gain for the feedback amplifier section was determined early in this phase of the circuit design. The difficult issues were how to provide for summing points for the amplified feedback signal and the reference input, such that they would not interfere with each other. This was dealt with during prototyping by providing an input preamplifier stage to the feedback and reference signals before the two were summed. The feedback preamplifier stage had a gain of 20, while the reference signal input required unity gain.

The LM301 operational amplifiers were eliminated from the final design because they required too much board space and were not internally compensated for frequency response. As the system was not expected to be run at very high frequencies, circuitry with adjustable frequency compensation was deemed unnecessary. In addition, during several instances in prototyping, the LM301 operational amplifier stages would apparently interact, lose stability and go into high frequency oscillation.

To simplify the amplifier design by reducing components, the four LM301 Operational Amplifiers needed at

the time were replaced by a single LM324 quad op amp that had the same high gain characteristics of the LM301 but included internal frequency compensation. This meant a minimal number of external components were necessary to support the IC. The LM324 was also found to provide a much more stable signal at high gain than did the series of LM301 ICs.

Adjustable input voltage offsets (potentiometer) were added to particular operational amplifiers to calibrate the zero position of the encoder. After a successful test of the feedback amplifier was achieved, the author considered ways to improve the feedback signal by stabilizing it very large gain.

During prototype tests with the LM301 op amps, however, the author found that at large preamplifier gains, the motor position would be unstable and the motor would vibrate at what appeared to be a natural resonant frequency of about 25 Hz. Several attempts were made to design circuitry to eliminate motor vibration at these upper gain levels. The first attempt was to insert a low pass filter inline with the preamplifier stages to suppress gain at frequencies above approximately 25 Hz. A standard design was adapted from Jung [Ref. 6, p. 498]. A copy of the low pass filter schematic and component values are provided in Appendix S.

The low pass filter was not successful in eliminating the vibration. The system response was decreased (no higher frequency response components), and the oscillations both grew larger in amplitude and shifted to lower frequencies.

A band-elimination filter to eliminate the 20-30 Hz range was considered briefly, but it was not actually implemented. It was felt that, if a 25 Hz excitation was placed on the servo system, it would not respond. Therefore, the design seemed unacceptable in this form and was not tested further.

A final effort at eliminating the oscillation was made with a differentiator circuit placed in a negative feedback arrangement in the preamplifier stages. The idea was to use the differentiator as a type of electronic "friction", as it would perform a differentiation of the voltage in the feedback loop. Differentiating the voltage analog of the system's "acceleration" produces a voltage analog of "velocity". As frictional torque is a velocity-dependent concept, it was felt that introduction of artificial friction into the system could cut down the Q of the oscillation, thereby stabilizing the response.

The attempt at a useful differentiator circuit is shown in Appendix T. The circuit design was adapted from Jung [Ref. 6, p. 365]. This circuit proved to be unsuccessful because of the discrete nature of the encoder

output. Each step in the encoder output resembles an infinite acceleration, and thus tends to drive the differentiator circuit into producing a delta function-type spike at its output.

After several unsuccessful attempts with the different feedback filter configurations, the LM324 Op Amps were introduced as mentioned above, which stabilized the feedback considerably. At this point, it was the author's judgement that boosting the high frequency components of the feedback signal would help better stabilize the motor as well as increase the overall system response.

A 100 Hz, two pole Butterworth high-pass filter design, adapted from Horowitz and Hill [Ref. 7, p. 274], was placed in the preamplifier stages. The high-pass signal was amplified and summed with the feedback signal at the point where it is fed to the motor power amplifier. This arrangement not only boosted the frequency response of the system to broad-band inputs such as square waves, but also served to stabilize the feedback loop.

c. Motor Power Amplifier Circuit

The author's original thoughts in the prototyping design of the LM12 power amplifier were to configure the IC in a high gain configuration, thus reducing the need for a complex system of preamplifiers. Many unsuccessful attempts were made to vary the feedback values to produce a stable motor drive signal. In every instance the LM12 output

suffered from high frequency, low-amplitude oscillations and instability. Reconfiguring the LM12 as a voltage follower with input compensation eliminated the problem. As part of the original prototype input compensation, a 5K ohm resistor was placed in parallel with a 200pf capacitor at the input to the LM12. During later system tests, the author found that removing the resistor/capacitor combination on the input boosted the gain of the system, while the output remained free of oscillation.

The early prototype design of the LM12 power operational amplifier circuit included a 5 ohm resistor and a 4μ henry inductor combination in series with the motor load. The manufacturer's data sheet for the LM12 recommended inclusion of these components to improve the amplifier's performance when driving highly reactive loads. During system tests the resistor value was repeatedly reduced by trial-and-error, and system performance improved with no side effects. During most of the prototype testing period, a 1 ohm high wattage output resistance was used. This resistance approximately halved the power delivered to the motor. Once final trimming of the amplifier's response was completed, the resistor/inductor combination was removed. The motor shaft torque dramatically increased as all of the circuit power was then available to the motor.

5. System Hardwiring

a. Circuit Boards

Following the prototype testing of the encoder analog conversion and amplifier circuits, a more permanent version of each circuit was assembled on a soldered circuit board. The operation of the completed boards was functionally identical to the circuits assembled on the protoboards. Screw lug terminals were attached to wires leading to and from the circuit boards to ease in maintenance. Pin-to-pin connections between ICs were done using above-board wire jumpers that were soldered on the under side of the board. The ICs were fixed to the board using appropriately sized solderless IC sockets. Photographs of the encoder analog conversion and amplifier circuit cards are provided in Figures 10 and 11.

After assembly, the circuit cards were mounted to the system plywood base using round head wood screws and aluminum standoffs. Lastly, the wires leading to and from the circuit cards were attached to terminal blocks also mounted on the plywood base.

Drawings of the component locations on each of the encoder DAC and feedback amplifier circuit cards are provided in Appendices U and V. All components which could require adjustment are identified as is the input/output wiring of the circuit cards.

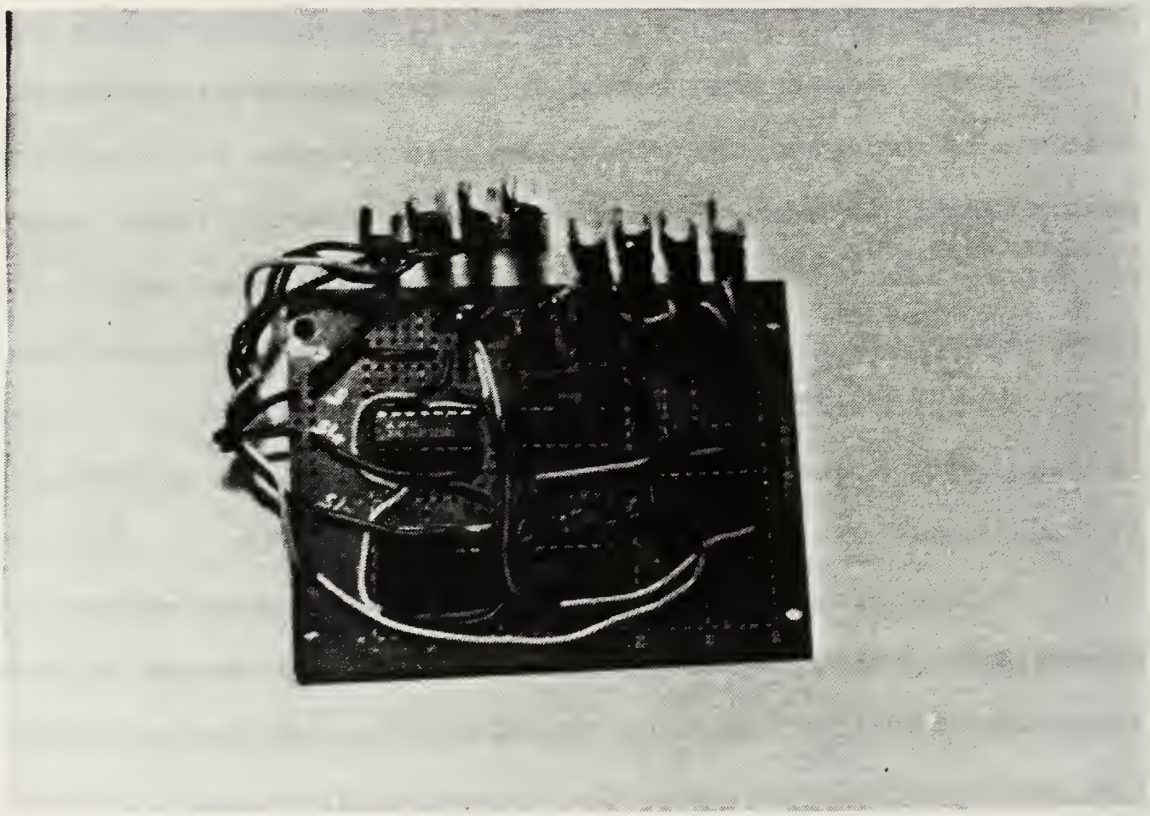

Figure 10
Photograph of Encoder Analog Conversion Card.

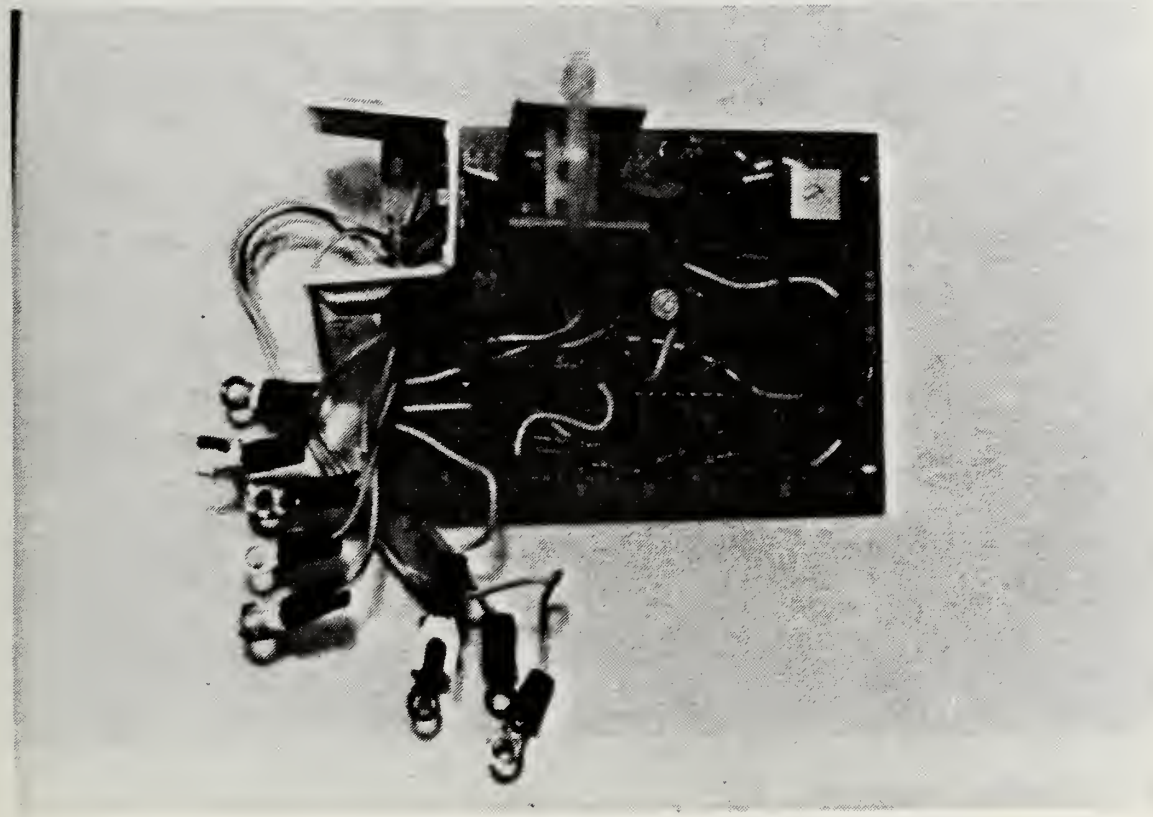

Figure 11
Photograph of Amplifier Circuit Card.

b. Motor Power Amplifier Circuit

The LM12 power operational amplifier and heat sink assembly discussed in the System Assembly section of this thesis was mounted to the plywood base. The LM12 pins on the underside of the heat sink were connected to a screw-type terminal block with 14 gauge wire. The additional circuitry comprised of output clamp diodes, supply voltage capacitors, and input compensation were mounted on the terminal block for accessibility. In a more permanent system, these components should be mounted as close as possible to the pins of the LM12 to further eliminate spurious oscillation problems.

c. Completed System Configuration

A photograph of the completed servo motor system is provided in Figure 12. The reference signal input was mounted in the front to the left of the motor-encoder cage with a BNC input connection. Supply voltage is routed to a terminal block mounted toward the rear.

E. SYSTEM TESTING

1. Preliminary Prototyping Setup Testing

a. Shaft position/feedback signal levels

The key to the performance and stability of the servo system was essentially the determination of the degree of feedback that corresponded to an incremental deviation in shaft position that registered as a change in the encoder's

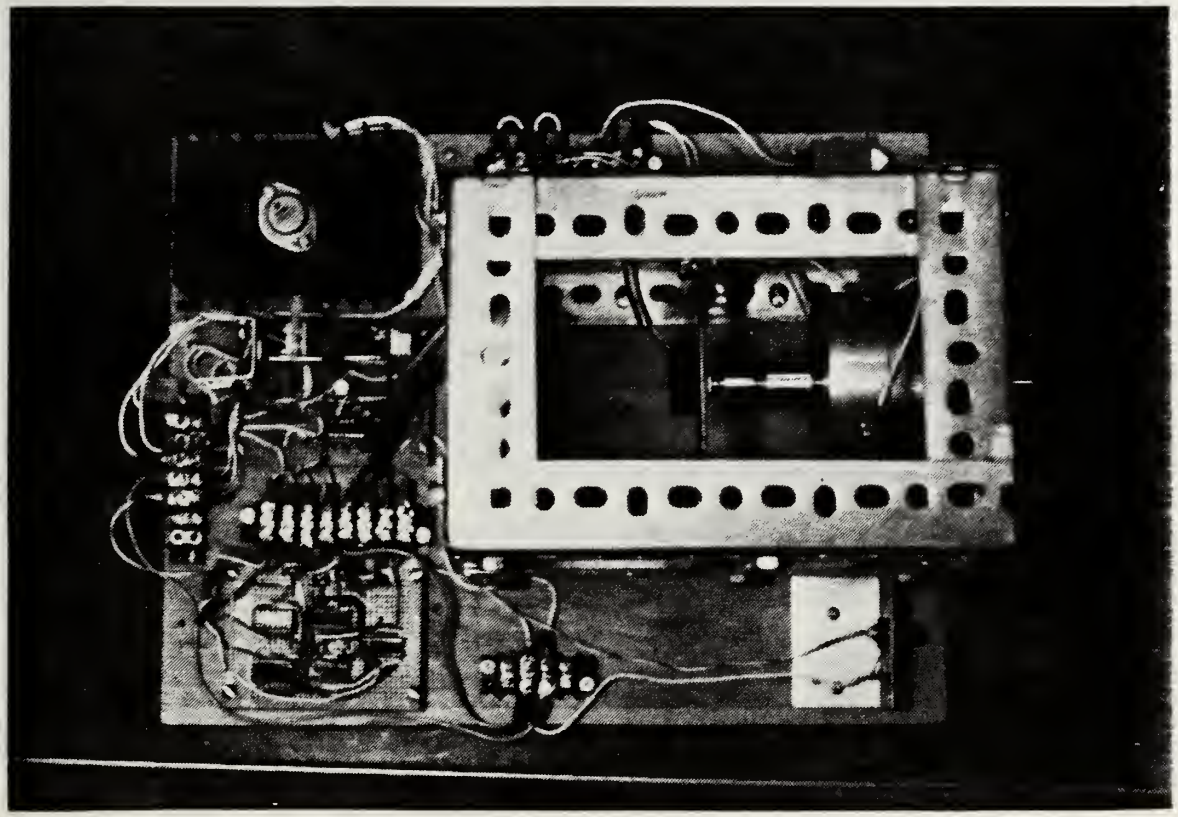

Figure 12
Photograph of Completed Motor Servo System

least significant bit (LSB). Through tests during the prototype development, the author found that the optimum setting of the feedback signal from the amplifier circuit to the motor power amplifier was ±5 volts for such a LSB change of the shaft encoder output (saturating at ±15 VDC). Any more amplification of the feedback signal would cause the system to behave like an undamped oscillator. In that configuration, the system would be metastable and break into oscillation at the slightest disturbance from its initial equilibrium state. The ± 5 VDC steps provided a sort of "potential well" where the motor could quickly and safely stabilize at its nominal position.

The test conducted to make the determination described above was fairly simple in nature. The voltage level of the feedback signal being fed to the motor power amplifier was monitored on a Tektronix Model 2336, 100 MHz oscilloscope like that shown in Figure 13.

A ±5 volt square wave signal was fed to the reference signal input port. While the motor was responding to the reference signal, the gain on the final stage of the amplifier circuit was increased by adjusting the board-mounted potentiometer. Once the system lost stability due to the increased gain, the potentiometer resistance was slightly reduced to the point where the response was consistently stable.

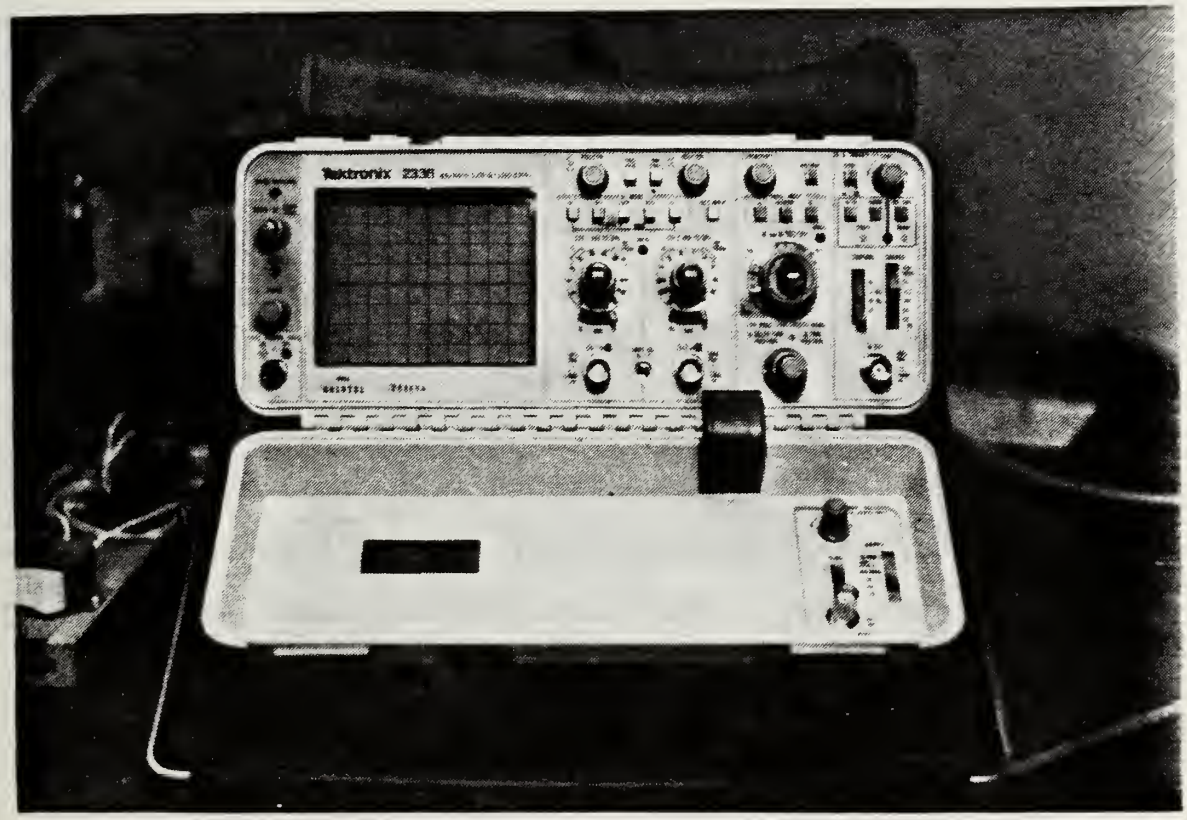

Figure 13
Photograph of Tektronix Model 2336 Oscilloscope

To determine the feedback voltage levels, the reference signal was removed. The motor was disabled with a switch in the wire between the motor's negative terminal and ground. The motor was turned by hand in order to vary its position by only a few positional bits in each direction while watching the voltage of the feedback signal on the oscilloscope. Thus the feedback voltage levels were noted.

Three conditions of gain versus system stability were measured and are presented graphically in Figure 14 to illustrate their relationship in the servo system. The first (top) line in the graph represents the gain which the system is metastable, i.e., any perturbation would set the motor into oscillation. The second line is the optimal gain condition at which the system has maximum torque and consistent stability. The third line represents the gain value at which the system response is significantly diminished. Due to the digital shaft encoder, the graph displays the discrete values of feedback gain versus rotational deviation.

Potential wells analogous to that of a damped harmonic oscillator are superimposed in dashed lines on the graph in Figure 14 to provide a correlation to the discrete system response. A steeper slope (high gain) corresponds to an underdamped motion; which, in the case of the servo system, results in metastable behavior. Slightly below the system's metastable gain region is the optimal operating

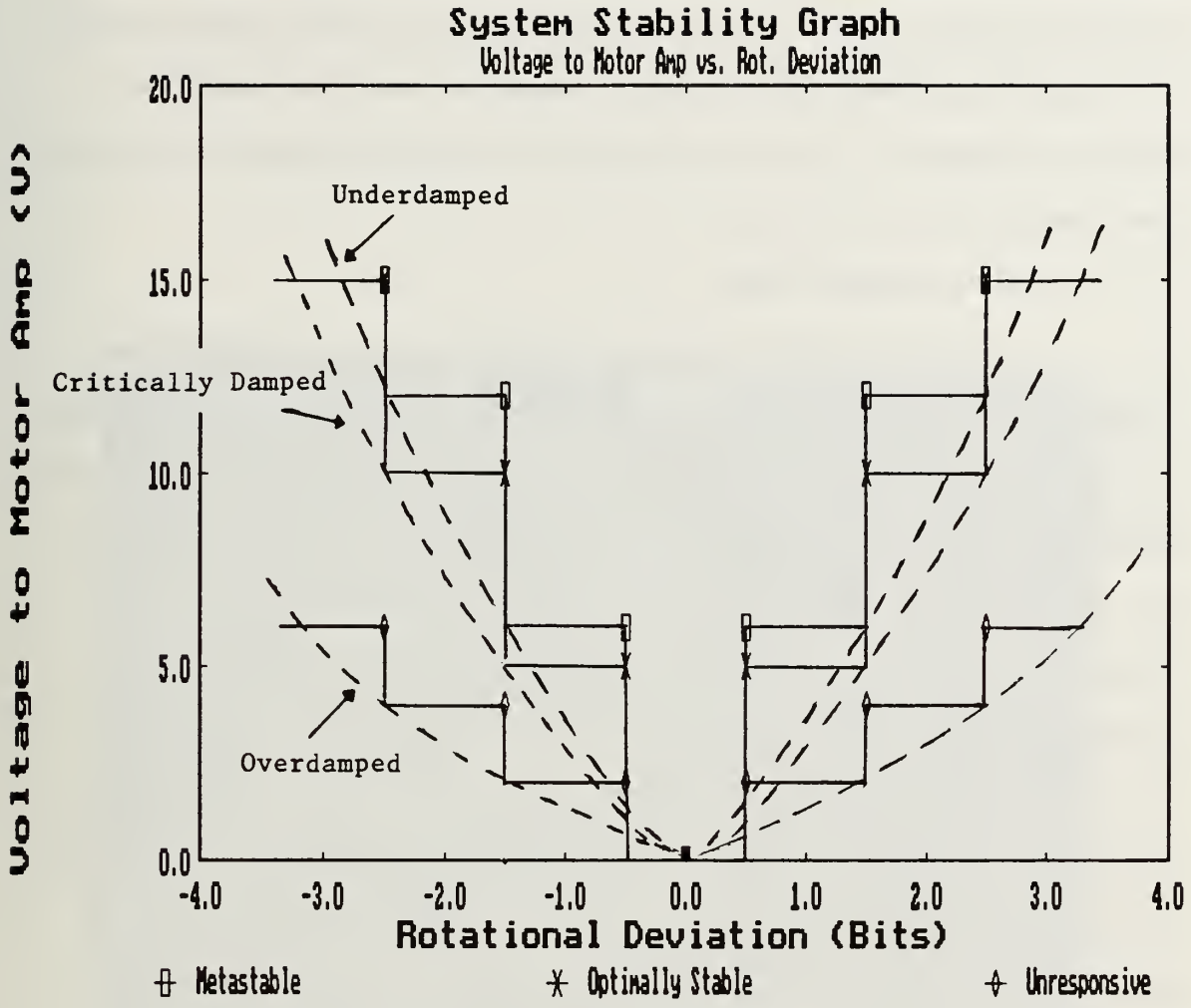

Dashed lines represent the underdamped, critically damped, and overdamped analogs of the simple harmonic oscillator with respect to the discrete potential wells plotted.

Figure 14
Graph of System Stability vs. Gain

condition. This is analogous to a critically damped harmonic oscillator. Further reduction of the system gain in turn diminishes the system response and the behavior becomes sloppy. This correlates to the overdamped motion of the harmonic oscillator.

2. Motor Speed Test

A motor speed test was conducted to ascertain a baseline performance measure of the system. A low frequency (5 Hz) square wave at approximately 2 volts peak-to-peak was used as the reference signal. The system response signal was taken from the output of the first stage of the amplifier circuit so that the response was adequately buffered by the amplifier stage.

The photograph of the oscilloscope trace (Figure 15) provides clear evidence of the superior speed and tracking ability of the feedback system. The dots in the system position response trace are the result of the discrete voltage output of the D-A converter in the Encoder Analog Conversion circuit. As 128 pulses are generated by the encoder per shaft revolution, each dot in the trace represents 360° /128, or approximately 2.8° of shaft movement. Counting the dots reveals that 36.4° of shaft movement occurred in 20 milliseconds. It is also noted that the shaft was locked into position within 40 milliseconds of arriving at the 1/e rise time position. Therefore, it is

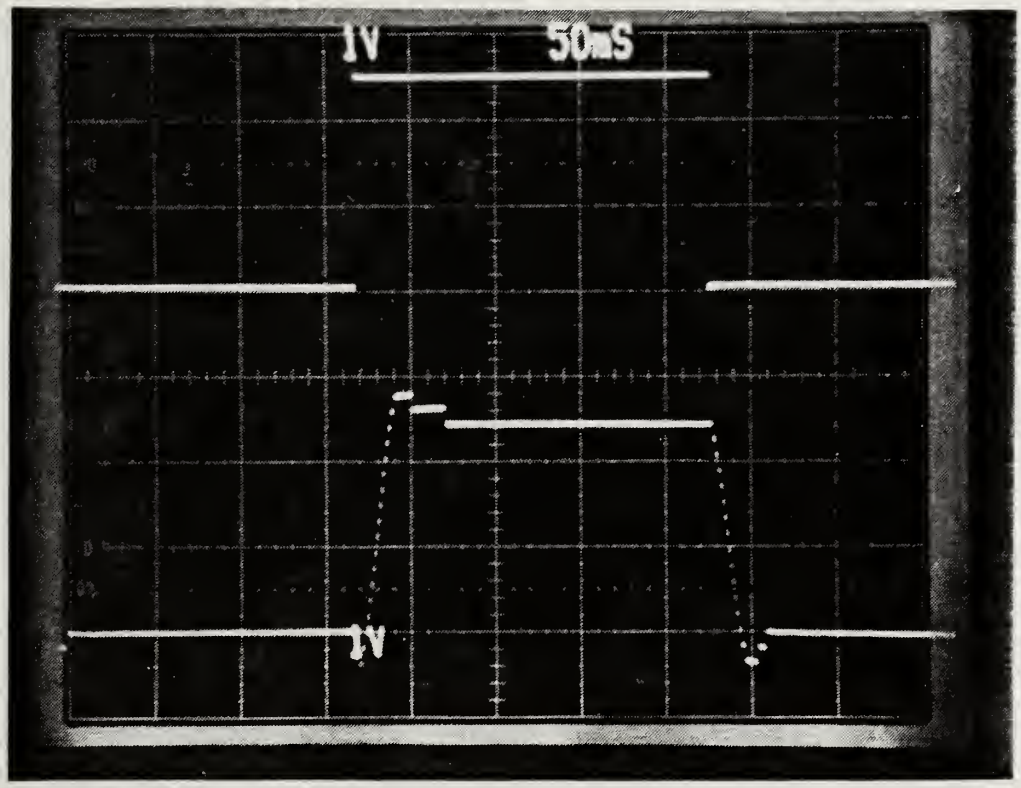

Figure 15
Servo Motor Speed Test - Oscilloscope Trace

safe to assume that the system response time constant falls in the 20 - 40 millisecond range, corresponding to a frequency bandwidth of 25 - 50 hertz.

3. Motor Torque Test

A test was conducted to determine the torque capability of the system under a static load. A torque test bar was designed as shown in Appendix W. A photograph of the test being conducted is provided in Figure 16. The motor supported a 250 gram load at a right angle to a moment arm of 10.0 cm for approximately 30 seconds. The torque of the system was therefore calculated to be 0.245 N-m. The power amplifier and heat sink were extremely hot after the test, but the system performance did not deteriorate.

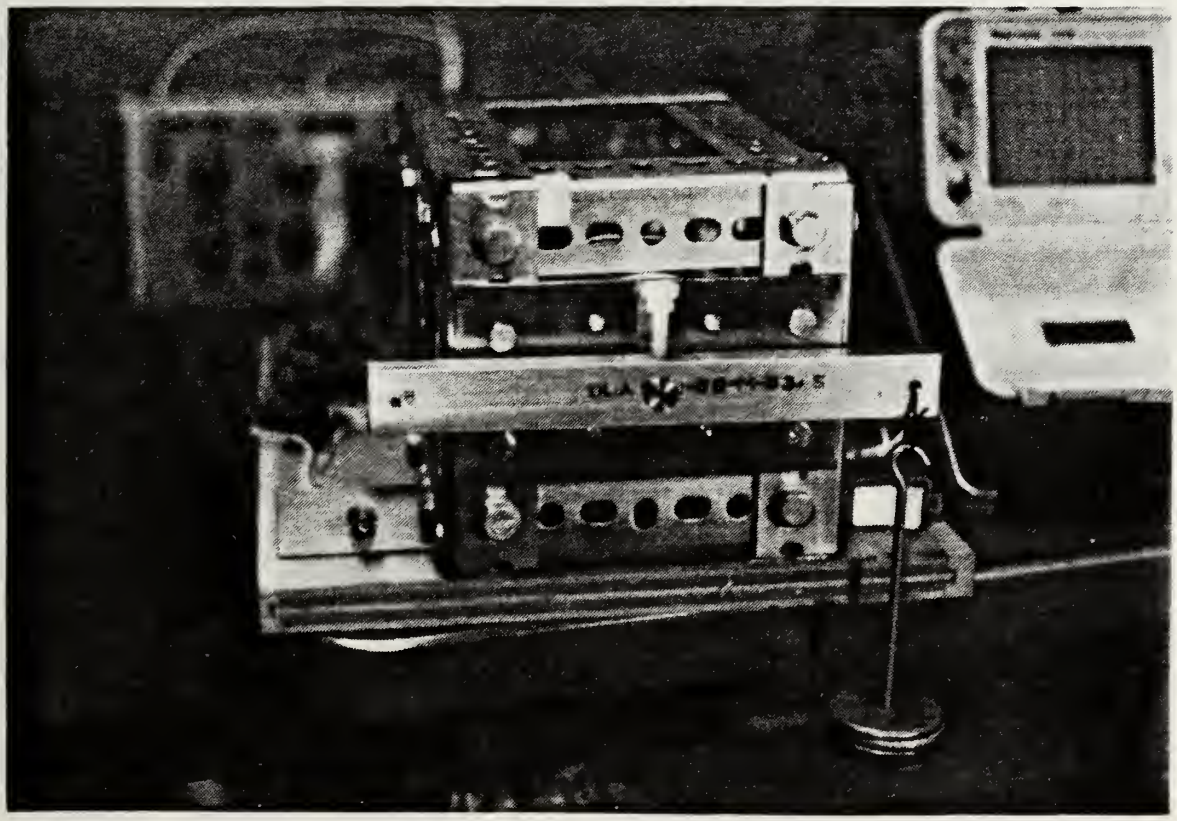

Figure 16
Photograph of Torque Test Setup

IV. SUGGESTIONS FOR FURTHER RESEARCH AND SYSTEM ENHANCEMENTS

The system fabricated under this thesis works superbly as designed. However, positioning the orthogonal function image mask to the resolution needed for the imaging system proposed by Davis will require a shaft position encoder with at least 100 times finer resolution.

Referring again to Figure 14, the discrete nature of the position encoder used in this thesis project would force the system to be metastable at gain levels much lower than that possible with an analog feedback system. The system behaves much like a marble in a box. The position of the marble in the box is difficult to stabilize if the box is disturbed. However, a marble placed in a smooth bowl and disturbed will inevitably return to the nominal (center) position. With proper damping, the marble will quickly settle on the nominal position.

To make the system behave in a similarly smooth manner as the marble in a bowl described above, an encoding scheme is under development in another thesis study to employ a phase-locked loop analog feedback system instead of the simple digital version employed in this thesis project. With the analog feedback, much greater system sensitivity will be possible. Likewise, it should be possible to

increase overall system gain once the transients associated with the current low resolution encoder are eliminated.

Future feedback system enhancements planned by Davis, such as using the differentiator feedback circuit to induce the artificial friction mentioned in section D.4.b., will also help stabilize the circuit at much larger feedback gain levels.

V. CONCLUSIONS

The development of a baseline, highly capable and upgradeable servo system for an imaging spectrometer system was successful. This thesis offers incontestable proof of the power, stability and precision of the servo system while utilizing a digital shaft encoder only accurate to ±1.5°. The exercise of developing a theoretical mathematical model of the system response proved extremely useful in understanding the system's actual behavior when reacting to a pulse-type voltage stimulus.

The work on this servo system, however, is far from complete. Following the development of an analog phase-locked loop system, the system will enjoy much higher gain in the feedback signal while maintaining excellent stability.

Reference List

1. NASA Space and Earth Sciences Advisory Council, *SOFIA: Stratospheric Observatory For Infrared Astronomy*, pp. 1-14, Ames Research Center, 24 May 1988.

2. Davis, D.S., "A New Technique for Efficient Multiplex Imaging and Imaging Spectroscopy," Paper in Preparation.

3. DiStefano III, J.J., Stubberud, A.R., Williams, I.J., *Schaum's Outline of Theory and Problems of Feedback and Control Systems*, McGraw-Hill Book Co., 1967.

4. Kuo, B.C., *Automatic Control Systems*, Englewood Cliffs, New Jersey: Prentice-Hall, Inc., 1987.

5. Rutkowski, G., *Handbook of Integrated-Circuit Operational Amplifiers*, Englewood Cliffs, New Jersey: Prentice-Hall, Inc., 1975.

6. Jung, W.G., *IC Op-Amp Cookbook*, Indianapolis, IN: Howard W. Sams & Co., Inc., 1974.

7. Horowitz, P. and Hill, W., *The Art of Electronics*, Cambridge: Cambridge University Press, 1989.

APPENDIX A

CALCULATION OF MOTOR RESPONSE TO PULSE WAVE

Define Variables

$L := .005 \cdot H$ $\quad J := .5 \cdot kg \cdot m^2$ $\quad K_f := 20 \cdot N \cdot m \cdot \frac{sec}{coul}$

$B := .1 \cdot N \cdot m \cdot sec$ $\quad R := 1 \cdot \Omega$ $\quad K_t := .05 \cdot N \cdot m \cdot \frac{sec}{coul}$

Derive Constants

$$A := \frac{B \cdot L + R \cdot J}{2 \cdot J \cdot L} \qquad C := \frac{\sqrt{(B \cdot L - R \cdot J)^2 - 4 \cdot J \cdot L \cdot K_t \cdot K_f}}{2 \cdot J \cdot L}$$

$mm := 8$ $\quad Ampl := 10 \cdot VOLT$ $\quad LL := 2^{mm}$

$A = 100.1 \cdot time^{-1}$

$C = 97.878 \cdot time^{-1}$

Define Convolution Terms

$q := 0 \,..\, (LL - 1)$ $\quad V(t) := if(|t| < .5, Ampl, 0 \cdot VOLT)$

Note q is time variable

$$G1_q := e^{-(A+C) \cdot q \cdot \frac{sec}{LL}} \qquad G2_q := e^{-(A-C) \cdot q \cdot \frac{sec}{LL}} \qquad VV_q := V\left[\frac{q}{LL}\right]$$

Derive Fourier Transform of Convolution Terms

$ddl := cfft(G1)$ $\quad dd2 := cfft(G2)$ $\quad f := cfft(VV)$

Multiply Transforms -> $\quad fconv1_q := f_q \cdot ddl_q \quad fconv2_q := f_q \cdot dd2_q$

Perform Inverse Fourier Transform $\quad TOL := .05$

$conv1 := icfft(fconv1)$ $\quad conv2 := icfft(fconv2)$

Calculate all response terms

$$Firstterm_q := \frac{K_t}{J \cdot L \cdot \left[A^2 - C^2\right]} \cdot \int_0^{\frac{q}{LL}} V(\tau)\, d\tau \cdot sec$$

$$X := \frac{K_t \cdot sec}{\sqrt{LL \cdot 2 \cdot J \cdot L \cdot C}}$$

$$Secondterm_q := \frac{X}{A + C} \cdot conv1_q \qquad Thirdterm_q := \frac{X}{A - C} \cdot conv2_q$$

$$\theta_q := Firstterm_q + Secondterm_q - Thirdterm_q$$

$\theta new_q := \theta_q - \theta_0$ <- This step was done to start at zero (round errors)

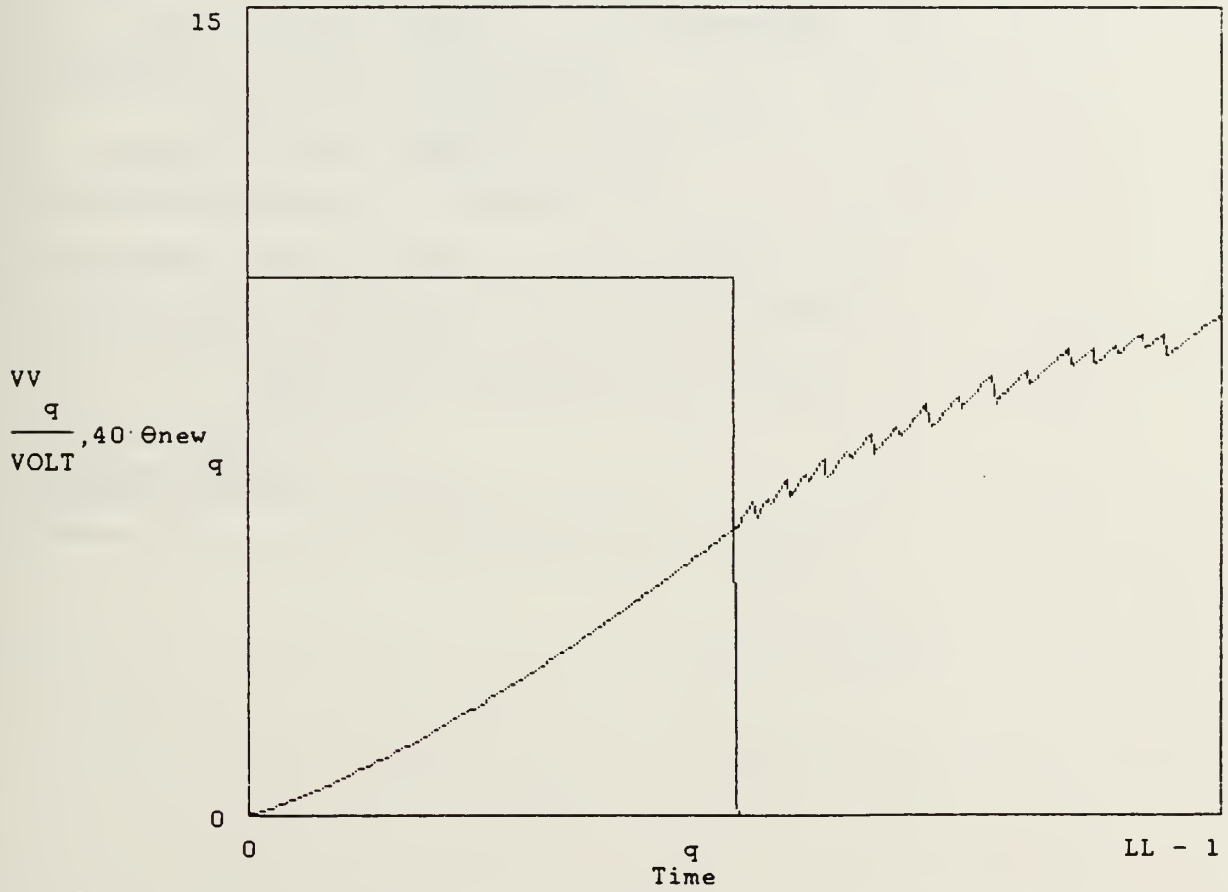

Plot of square voltage pulse on motor to motor angular response

Define units

$m \equiv 1L$ $\quad sec \equiv 1T$ $\quad coul \equiv 1Q$ $\quad kg \equiv 1M$

$$N \equiv \frac{kg \cdot m}{sec^2} \qquad H \equiv \frac{kg \cdot m^2}{coul^2} \qquad F \equiv \frac{coul^2 \cdot sec^4}{kg \cdot m^2} \qquad \Omega \equiv \frac{kg \cdot m^2}{sec \cdot coul^2}$$

$$JOULE \equiv N \cdot m \qquad AMP \equiv \frac{coul}{sec} \qquad VOLT \equiv \frac{kg \cdot m^2}{sec^2 \cdot coul} \qquad \mho \equiv \frac{m}{sec}$$

HI-TORQUE
PM FIELD
SERVO
12 VOLTS DC
1800 RPM

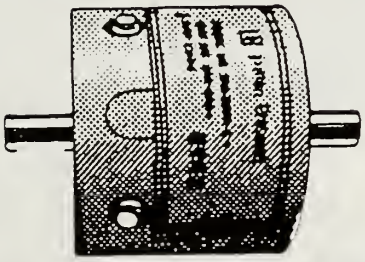

Clifton Precision #DH-3250-C-1 . . . Dual shaft (ball bearing). Technical specifications:

Peak Torque	**100 In-oz. at 12 Amps max.**
Continuous Torque	**38 In-oz max.**
Rotor Inertia	**0.0038 In-oz per sec^2**
Torque Constant	**8.55 In-oz/Amp**
Terminal Resistance	**1.1 Ohms**

Dual shafts 1/2 dia. x 0.937" and 0.88". Shaft end mounting with three tapped 6/32 holes at one end and four 8/32 tapped holes at opposite end. Motor 3.25" dia. x 2.875" long. Screw terminals. New. Shpg Wt, 5 lbs.

TM89MTR5615 _____

National Semiconductor

LM12 (L/C/CL) 150W Operational Amplifier

General Description

The LM12 is a power op amp capable of driving ±35V at ±10A while operating from ±40V supplies. The monolithic IC can deliver 150W of sine wave power into a 4Ω load with 0.01% distortion. Power bandwidth is 60 kHz. Further, a peak dissipation capability of 800W allows it to handle reactive loads such as transducers, actuators or small motors without derating. Important features include:

- input protection
- controlled turn on
- thermal limiting
- overvoltage shutdown
- output-current limiting
- dynamic safe-area protection

The IC delivers ±10A output current at any output voltage yet is completely protected against overloads, including shorts to the supplies. The dynamic safe-area protection is provided by instantaneous peak-temperature limiting within the power transistor array.

The turn-on characteristics are controlled by keeping the output open-circuited until the total supply voltage reaches 14V. The output is also opened as the case temperature exceeds 150°C or as the supply voltage approaches the BV_{CEO} of the output transistors. The IC withstands overvoltages to 100V.

This monolithic op amp is compensated for unity-gain feedback, with a small-signal bandwidth of 700 kHz. Slew rate is 9V/μs, even as a follower. Distortion and capacitive-load stability rival that of the best designs using complementary output transistors. Further, the IC withstands large differential input voltages and is well behaved should the common-mode range be exceeded.

The LM12 establishes that monolithic ICs can deliver considerable output power without resorting to complex switching schemes. Devices can be paralleled or bridged for even greater output capability. Applications include operational power supplies, high-voltage regulators, high-quality audio amplifiers, tape-head positioners, x-y plotters or other servo-control systems.

The LM12 is supplied in a four-lead, TO-3 package with V^- on the case. A gold-eutectic die-attach to a molybdenum interface is used to avoid thermal fatigue problems. Two voltage grades are available; both are specified for either military or commercial temperature range.

Connection Diagram

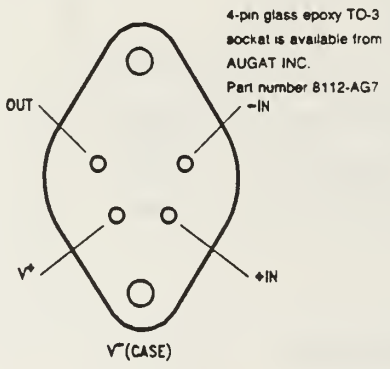

TL/H/8704–1

Bottom View

Order Number LM12K, LM12CK or LM12CLK
See NS Package Number K04A

Typical Application*

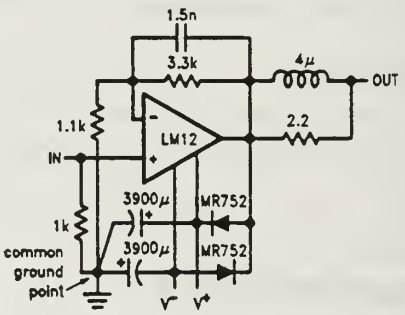

TL/H/8704–2

*Low distortion (0.01%) audio amplifier

Absolute Maximum Ratings

If Military/Aerospace specified devices are required, please contact the National Semiconductor Sales Office/Distributors for availability and specifications.

Total Supply Voltage	LM12/LM12C	100V
	LM12L/LM12CL	80V
Input Voltage		Note 1
Output Current		Internally Limited
Junction Temperature		Note 2
Storage Temperature Range		−65°C to 150°C
Lead Temperature (Soldering, 10 seconds)		300°C

ESD Rating to be Determined.

Operating Ratings

Total Supply Voltage	LM12/LM12C	15V to 80V
	LM12L/LM12CL	15V to 60V

Electrical Characteristics (Note 3)

Parameter	Conditions	Typ 25°C	LM12 LM12L Limits	LM12C LM12CL Limits	Units
Input Offset Voltage	$\pm 10V \le V_S \le \pm 0.5\ V_{MAX}$, $V_{CM} = 0$	2	7/**15**	15/**20**	mV (max)
Input Bias Current	$V^- + 4V \le V_{CM} \le V^+ - 2V$	0.15	0.3/**1.0**	0.7/**1.0**	μA (max)
Input Offset Current	$V^- + 4V \le V_{CM} \le V^+ - 2V$	0.03	0.1/**0.3**	0.2/**0.3**	μA (max)
Common Mode Rejection	$V^- + 4V \le V_{CM} \le V^+ - 2V$	86	75/**70**	70/**65**	dB (min)
Power Supply Rejection	$V^+ = 0.5\ V_{MAX}$, $-6V \ge V^- \ge -0.5\ V_{MAX}$	90	75/**70**	70/**65**	dB (min)
	$V^- = -0.5\ V_{MAX}$, $6V \le V^+ \le 0.5\ V_{MAX}$	110	80/**75**	75/**70**	dB (min)
Output Saturation Threshold	t_{ON} = 1 ms, ΔV_{IN} = 5 (**10**) mV, I_{OUT} = 1A	1.8	2.2/**2.5**	2.2/**2.5**	V (max)
	8A	4	5/**7**	5/**7**	V (max)
	10A	5	8		V (max)
Large Signal Voltage Gain	t_{ON} = 2 ms, V_{SAT} = 2V, I_{OUT} = 0	100	50/**30**	30/**20**	V/mV (min)
	V_{SAT} = 8V, R_L = 4Ω	50	20/**15**	15/**10**	V/mV (min)
Thermal Gradient Feedback	P_{DISS} = 50W, t_{ON} = 65 ms	30	50	100	μV/W (max)
Output-Current Limit	t_{ON} = 10 ms, V_{DISS} = 10V	13	16	16	A (max)
	t_{ON} = 100 ms, V_{DISS} = 58V	1.5	1.0/**0.6**	0.9/**0.6**	A (min)
		1.5	1.7	1.7	A (max)
	LM12/LM12C t_{ON} = 100 ms, V_{DISS} = 78V	0.7	0.6/**0.4**	0.5/**0.35**	A (min)
Power Dissipation Rating	t_{ON} = 100 ms, V_{DISS} = 20V	100	90/**40**	80/**55**	W (min)
	V_{DISS} = 58V	80	58/**35**	52/**35**	W (min)
DC Thermal Resistance	(Note 4) V_{DISS} = 20V	2.3	2.6	2.9	°C/W (max)
	V_{DISS} = 58V	2.7	4.0	4.5	°C/W (max)
AC Thermal Resistance	(Note 4)	1.6	1.9	2.1	°C/W (max)
Supply Current	V_{OUT} = 0, I_{OUT} = 0	60	80/**90**	120/**140**	mA (max)

Note 1. Neither input should exceed the supply voltage by more than 50 volts nor should the voltage between one input and any other terminal exceed 80 volts for the LM12/LM12C or 60 volts for the LM12L/LM12CL.

Note 2. Operating junction temperature is internally limited near 225°C within the power transistor and 160°C for the control circuitry.

Note 3. The supply voltage is ±40V (V_{MAX} = 80V) for the LM12/LM12C and ±30V (V_{MAX} = 60V) for the LM12L/LM12CL, unless otherwise specified. The voltage across the conducting output transistor (supply to output) is V_{DISS} and internal power dissipation is P_{DISS}. Temperature range is $-55°C \le T_C \le 125°C$ for the LM12/LM12L and $0°C \le T_C \le 70°C$ for LM12C/LM12CL, where T_C is the case temperature. Standard typeface indicates limits at 25°C while boldface type refers to limits or special conditions over full temperature range. With no heat sink, the package will heat at a rate of 35°C/sec per 100W of internal dissipation.

Note 4. This thermal resistance is based upon a peak temperature of 200°C in the center of the power transistor and a case temperature of 25°C measured at the center of the package bottom. The maximum junction temperature of the control circuitry can be estimated based upon a dc thermal resistance of 0.9°C/W or an ac thermal resistance of 0.6°C/W for any operating voltage.

Although the output and supply leads are resistant to electrostatic discharges from handling, the input leads are not. The part should be treated accordingly.

INTERNATIONAL SERIES DESCRIPTION

The INTERNATIONAL SERIES is a high reliability line of open-frame power supplies designed to operate from the wide range of AC power sources found worldwide.

This feature greatly simplifies your inventory and service considerations by allowing the use of one standard power supply regardless of destination.

Additionally, these models are designed to meet domestic and European regulatory agency requirements.

If you plan to distribute your products worldwide, obtaining necessary agency approvals can be greatly simplified by specifying POWER-ONE, INC. INTERNATIONAL SERIES.

Power-One
D.C. POWER SUPPLIES

INTERNATIONAL SERIES DC POWER SUPPLIES

DRAWING NO. 51281 REV. L

SPECIFICATIONS AND APPLICATION DATA

VOLTAGE/CURRENT RATING CHART

MODEL	+2V	+5V	+12V	+15V	+18-20V	+24V	+28V	-5V	-12V	-15V	-18-20V	-24V	CASE
SINGLE OUTPUT													
HA5-1.5/OVP-A		1.5											B
HA15-0.9-A			0.9 or 0.9										B
HA24-0.5-A						0.5 or 0.5							B
H82-3-A	3.0												B
H85-3/OVP-A		3.0											B
HB12-1.7-A			1.7										B
HB15-1.5-A				1.5									B
HB24-1.2-A						1.2							B
HB28-1-A							1.0						B
HC2-6-A	6.0												C
HC5-6/OVP-A		6.0											C
HC12-3.4-A			3.4										C
HC15-3-A				3.0									C
HC24-2.4-A						2.4							C
HC28-2-A							2.0						C
HD2-12-A	12.0												D
HD5-12/OVP-A		12.0											D
HD12-6.8-A			6.8										D
HD15-6-A				6.0									D
HD24-4.8-A						4.8							D
HD28-4-A							4.0						D
HE2-18-A	18.0												E
HE5-18/OVP-A		18.0											E
HE12-10.2-A			10.2										E
HE15-9-A				9.0									E
HE24-7.2-A						7.2							E
HE28-6-A							6.0						E
HN5-9/OVP-A		9.0											N
HN12-5.1-A			5.1										N
HN15-4.5-A				4.5									N
HN24-3.6-A						3.6							N
HN28-3-A							3.0						N
DUAL OUTPUTS													
HAA5-1.5/OVP-A		1.5						1.5					AA
HAA15-0.8-A			1.0 or 0.8					-0.4 or 1.0 or 0.8					AA
HAA24-0.6-A					0.4 or 0.6						0.4 or 0.6		AA
HAA512-A		2.0	▽0.5 or ▽0.5										AA
HAD12-0.4-A			0.4						0.4				B
HAD15-0.4-A				0.4						0.4			B
HBB5-3/OVP-A		3.0						3.0					BB
HBB15-1.5-A			1.7 or 1.5					-0.7 or 1.7 or 1.5					BB
HBB24-1.2-A					0.9 or 1.2						0.9	1.2	BB
HBB512-A		3.0	▽1.25 or ▽1.25										BB
HCC5-6/OVP-A		6.0						6.0					CC
HCC15-3-A			3.4 or 3.0						3.4 or 3.0				CC
HCC24-2.4-A					1.8 or 2.4						1.8 or 2.4		CC
HCC512-A		6.0	▽2.5 or ▽2.5										CC
HDD15-5-A			5.0 or 5.0						5.0 or 5.0				E
TRIPLE OUTPUTS													
HTAA-16W-A		2.0	0.4 or 0.4					-0.4 or ▽0.4 or ▽0.4					AA
HBAA-40W-A		3.0	1.0 or 0.8					-0.4 or 1.0 or 0.8					BAA
HCAA-60W-A		6.0	1.0 or 1.0					-0.4 or 1.0 or 1.0					O
HCBB-75W-A		6.0	1.7 or 1.5					-0.7 or 1.7 or 1.5					CBB
HDBB-105W-A		12.0	1.7 or 1.5					-0.7 or 1.7 or 1.5					DBB
CP131-A		8.0	1.7 or 1.5					-0.7 or 1.7 or 1.5					131

HIGH VOLTAGE

MODEL	±48V	±120V	±180V	±200V	±250V	CASE
HB48-0.5-A	0.5					B
HC48-1-A	1.0					C
HD48-3-A	3.0					O
HE48-4-A	4.0					E
HB120-0.2-A		0.2				B
HB200-0.12-A ⸗			0.12 or 0.12			B
HB250-0.1-A					0.1	B

- ▪ −12V(or −15V) requires jumper on PCB for −5V.
- † for ±12V, refer to chassis silkscreen.
- ⸗ for 180V, refer to chassis silkscreen.
- ▼ 12V to 15V adjustable output
- ___ indicates no remote sense.

Specifications subject to change without notice.

FEATURES

- VDE transformer construction
- ±.05% regulation.
- T.C. burned-in to MIL-883 Lev. B
- Chassis notched for AC input
- 100/120/220/230-240 VAC
- Industry standard size
- Full rated to 50°C
- Remote sense - most outputs
- UL recognized/CSA certified
- OVP on 5V outputs
- 2 hour burn-in period
- Foldback/current limit

SPECIFICATIONS

AC INPUT: 100/120/220/230-240 VAC, +10%, -13%, 47-63Hz (Derate output current 10% for 50 Hz operation.) See AC connection table under APPLICATION NOTES for jumper information. Fuse information is next to outline and mounting drawings.

DC OUTPUT: See Voltage/Current Rating Chart. Adjustment range ±5% minimum. (Voltage nonadjustable on HAD models.)

LINE REGULATION: ±.05% for a 10% line change. (±1% for HAD models.)

LOAD REGULATION: ±.05% for a 50% load change. (±1% for HAD models.)

OUTPUT RIPPLE: 2V to 15V outputs: 5.0mV PK-PK maximum.
24V to 250V outputs: 3.0mV+.02%Vout Pk-Pk maximum.
(HAD models: 0.1%Vout Pk-Pk maximum.)

TRANSIENT RESPONSE: ≤50us for a 50 to 100% load change.

SHORT CIRCUIT AND OVERLOAD PROTECTION: Automatic current limit/foldback.

OVERVOLTAGE PROTECTION: Built-in on all 5V outputs. Set at 6.2VDC ±0.4V. Other outputs may use optional overvoltage protection.

REMOTE SENSING: Provided on most models, open sense lead protection built-in.

STABILITY: ±0.3% for 24 hour period after 1 hour warm-up.

TEMPERATURE RATING: 0°C to 50°C full-rated, derated linearly to 40% at 70°C. 12 CFM forced air cooling required to meet IEC 380/950 above 80% of total rated output power.

TEMPERATURE COEFFICIENT: ±.03%/°C maximum.

EFFICIENCY: (typical) 2V to 5V outputs: 45%
12V and 15V outputs: 55%
24V through 28V & 48V through 250V outputs: 60%

VIBRATION: Per MIL-STD-8100, Method 514.3, Category 1, Procedure I.

SHOCK: Per MIL-STD-8100, Method 516.3, Procedure III.

▪ Tolerance for 230VAC operation is +15%, -10%.
Note: specifications subject to change without notice.

WARRANTY

POWER-ONE, INC. warrants each power supply of its manufacture that does not perform to published specifications, as a result of defective materials or workmanship, for a period of two (2) full years from the date of original delivery.

POWER-ONE, INC. assumes no liabilities for the consequential damages of any kind through the use or misuse of its products by the purchaser or others. No other obligations or liabilities are expressed or implied.

PRODUCTS RETURNED FOR REPAIR

Please follow this procedure when returning products for servicing:

1. Contact Power-One's Customer Service Department for authorization to return products:

   POWER-ONE, INC.
   740 Calle Plano
   Camarillo, CA 93012
   USA

   PHONE: (805) 987-8741
   (800) 678-9445
   FAX: (805) 388-0476
   TWX: 910-336-1297

2. A Returned Material Authorization (RMA) will be issued and must appear on all shipping documents and containers.

3. Products must be returned freight pre-paid. Products returned freight collect or without an RMA number will be rejected and returned freight collect.

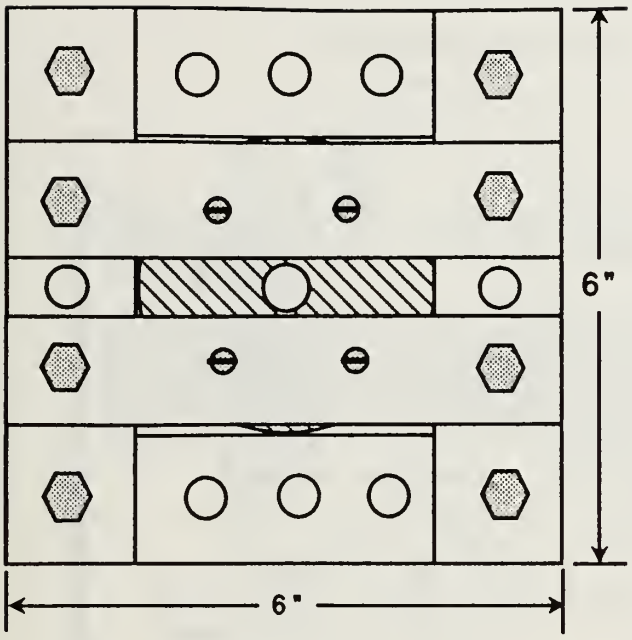

FRONT VIEW

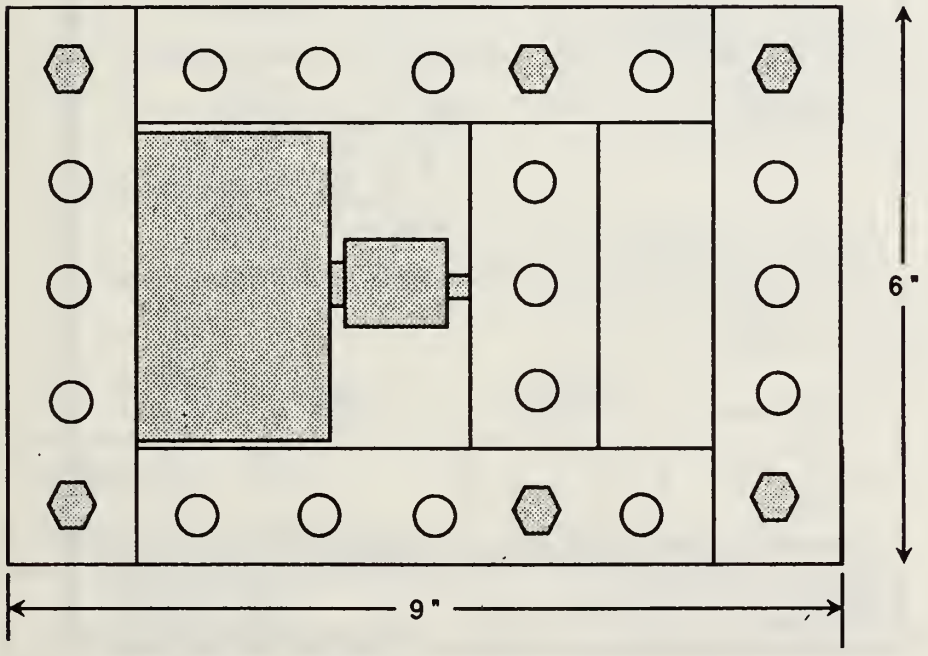

SIDE VIEW

Motor-Encoder Enclosure
Navy Postgraduate School Monterey, CA J. P. Sargent 9/3/91

SERIES:
600
601H
601V

OPTICAL ROTARY ENCODER

CLAROSTAT

ELECTRICAL SPECIFICATIONS: Description: The Series 600 and 601 controls are manually operated, rotary, optical encoders that output two square waves in quadrature at a rate of 128 pulses per channel per revolution as a standard with other resolutions down to 60 pulses available. The outputs are TTL compatible. The variation by series is the terminal configuration, with the Model 600 having 141 cable leads, and the Model 601 having 141 pin leads and internal resistors. Input Power: 4 volts DC ± 5% @ 30 MA max. plus external requirements. Output Rate: 128 pulses/revolution per channel standard. Channels: Two separate output channels in quadrature, 90° ± 45° Output Voltage: High level voltage – 2.4 volts min. with 10KΩ load to ground. Low level voltage – .4 volt max. **ENVIRONMENTAL CHARACTERISTICS:** Operating Temp.: – 20°C to + 65°C. **MECHANICAL CHARACTERISTICS:** Shaft Rotation: Continuous in either direction, 300 RPM max. Terminals: PC Type: .025 by .012 thick brass, gold plated to facilitate soldering. Cable Type: Four lead ribbon cable, color-coded, with .050 spacing, 28 AWG stranded copper wire, .039 diameter. Strength: Terminals withstand 2 lb. push and pull and a 90° bend.

CABLE CODE	
Color	**Function**
Red	5VDC ±5% @ 30 MA max.
Green	Ground
Yellow	A Out
Orange	B Out

MODEL 600 — CABLE STYLE

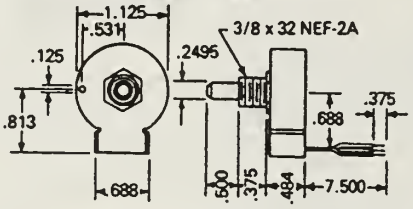

TERM #	FUNCTION
1	5VDC ±5% @ 30 MA max.
2	A Out
3	Ground
4	B Out

MODEL 601 — PC TERMINAL (HORIZONTAL)

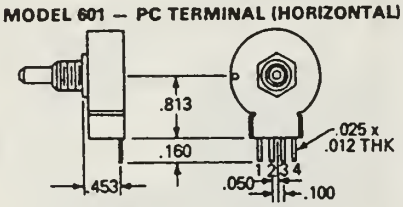

TERM #	FUNCTION
1	5VDC ±5% @ 30 MA max.
2	A Out
3	Ground
4	B Out

MODEL 601 — PC TERMINAL (VERTICAL)

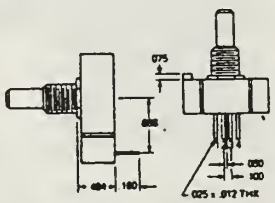

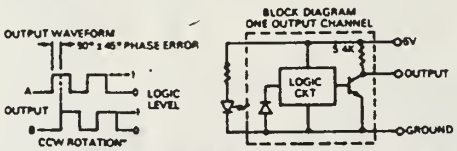

Digi-Key Part No.	Description	Price	Clarostat Part Number
600CS-ND	Cable Version	26.33	600-128-CBL
601HCS-ND	Horizontal PC Version	25.28	600-128-B66
601VCS-ND	Vertical PC Version	24.95	600-128-C24

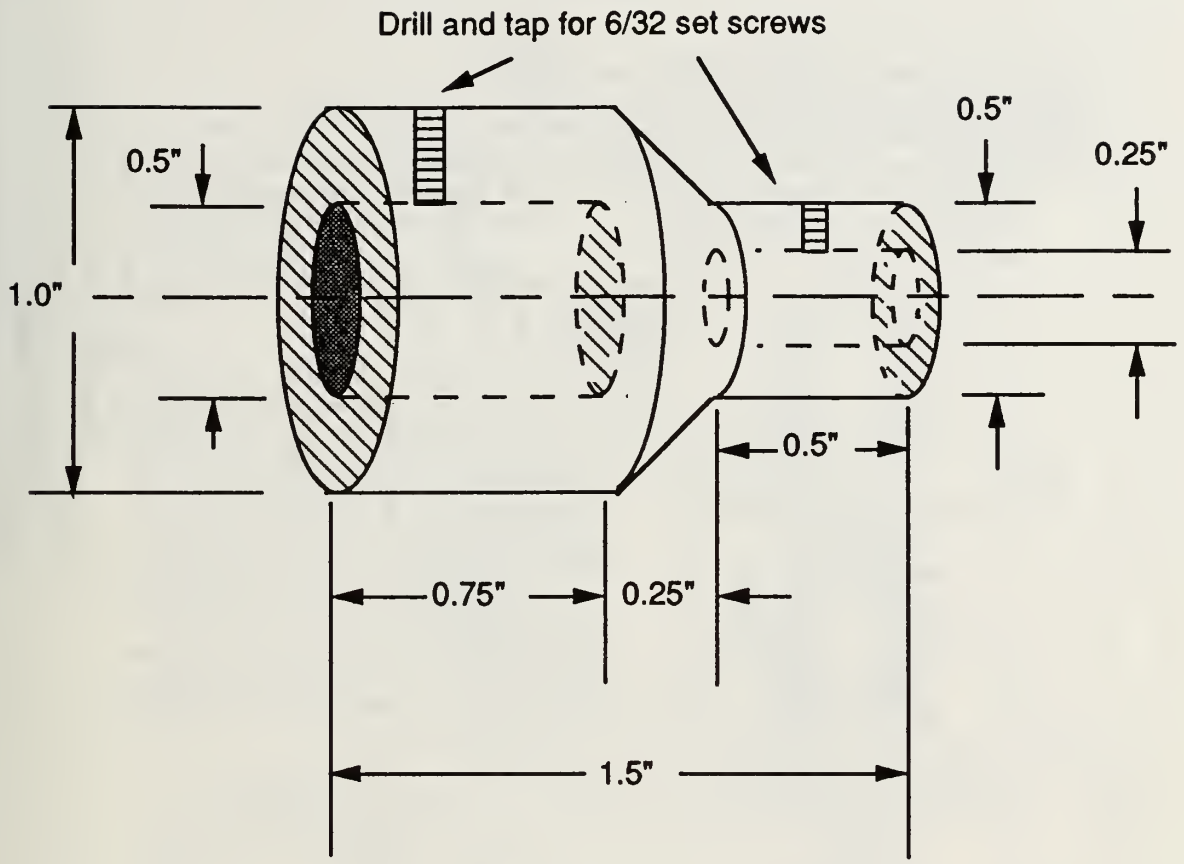

Scale 2:1

Notes

1. Make from 1" Aluminum Stock

2. Place holes for set screws 1/4" from ends.

Motor - Encoder Coupling

Navy Postgraduate School
Monterey, CA

J. P. Sargent 9-5-91

APPENDIX H

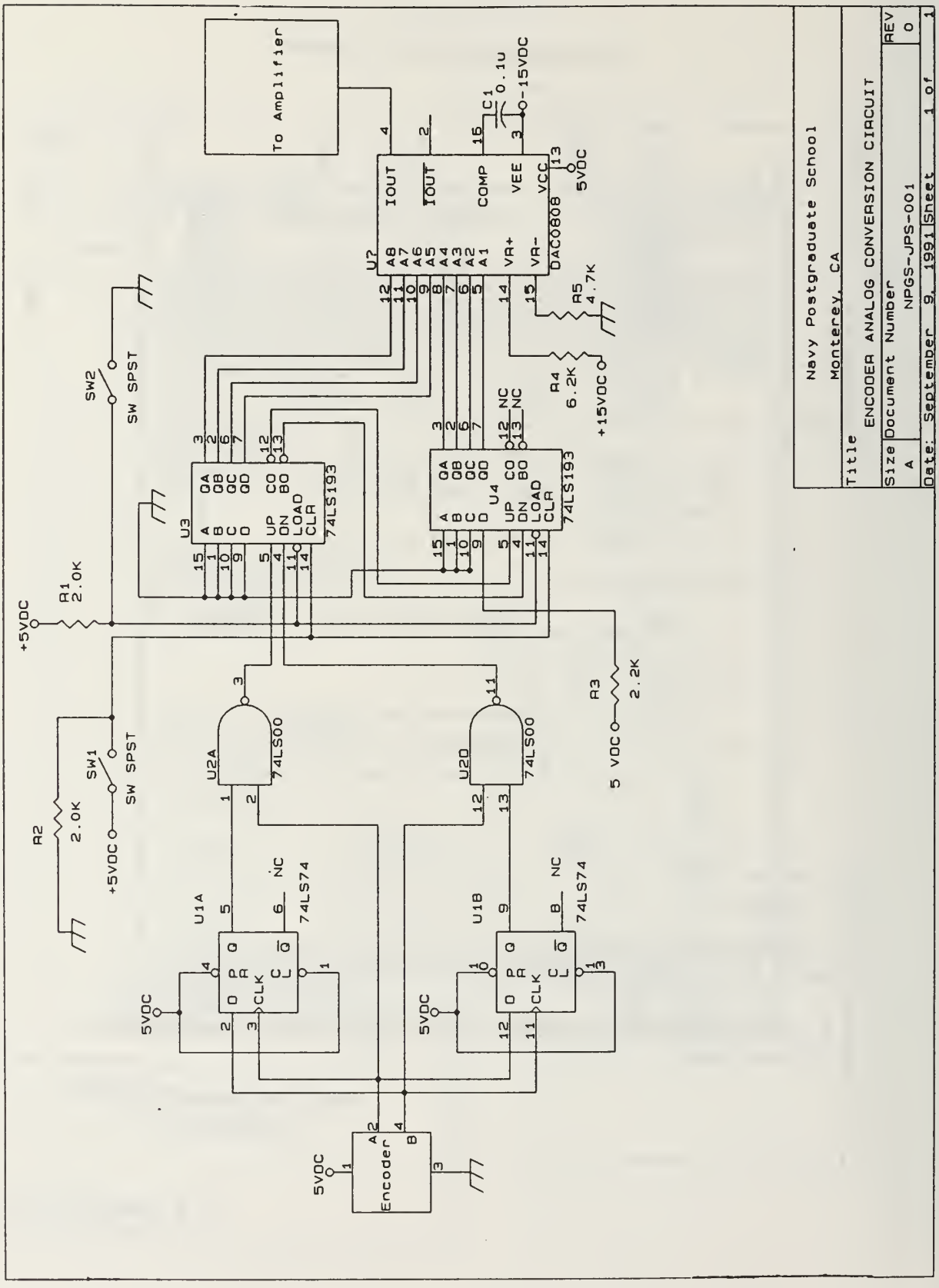
To Amplifier
U2
DAC0808
IOUT
IOUT
COMP
VEE
VCC
VR+
VR-
C1
0.1u
-15VDC
5VDC
R5
4.7K
R4
6.2K
+15VDC
SW2
SW SPST
SW1
SW SPST
R1
2.0K
+5VDC
R2
2.0K
+5VDC
R3
2.2K
5 VDC
U3
74LS193
U4
74LS193
U2A
74LS00
U2D
74LS00
U1A
74LS74
U1B
74LS74
Encoder
Navy Postgraduate School
Monterey, CA
Title
ENCODER ANALOG CONVERSION CIRCUIT
Size
A
Document Number
NPGS-JPS-001
REV
0
Date: September 9, 1991
Sheet 1 of 1

TYPES SN5474, SN54H74, SN54L74, SN54LS74A, SN54S74, SN7474, SN74H74, SN74LS74A, SN74S74
DUAL D-TYPE POSITIVE-EDGE-TRIGGERED FLIP-FLOPS WITH PRESET AND CLEAR

REVISED DECEMBER 1983

- **Package Options Include Both Plastic and Ceramic Chip Carriers in Addition to Plastic and Ceramic DIPs**
- **Dependable Texas Instruments Quality and Reliability**

description

These devices contain two independent D-type positive-edge-triggered flip-flops. A low level at the preset or clear inputs sets or resets the outputs regardless of the levels of the other inputs. When preset and clear are inactive (high), data at the D input meeting the setup time requirements are transferred to the outputs on the positive-going edge of the clock pulse. Clock triggering occurs at a voltage level and is not directly related to the rise time of the clock pulse. Following the hold time interval, data at the D input may be changed without affecting the levels at the outputs.

The SN54' family is characterized for operation over the full military temperature range of −55°C to 125°C. The SN74' family is characterized for operation from 0°C to 70°C.

FUNCTION TABLE

INPUTS				OUTPUTS	
$\overline{PRE}$	$\overline{CLR}$	CLK	D	Q	$\overline{Q}$
L	H	X	X	H	L
H	L	X	X	L	H
L	L	X	X	H†	H†
H	H	↑	H	H	L
H	H	↑	L	L	H
H	H	L	X	Q_0	$\overline{Q}_0$

† The output levels in this configuration are not guaranteed to meet the minimum levels for V_{OH} if the lows at preset and clear are near V_{IL} maximum. Furthermore, this configuration is nonstable; that is, it will not persist when either preset or clear returns to its inactive (high) level.

logic symbol

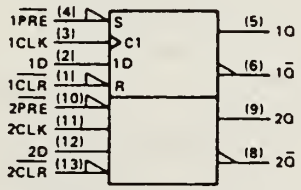

Pin numbers shown on logic notation are for D, J or N packages.

SN5474, SN54H74, SN54L74 . . . J PACKAGE
SN54LS74A, SN54S74 . . . J OR W PACKAGE
SN7474, SN74H74 . . . J OR N PACKAGE
SN74LS74A, SN74S74 . . . D, J OR N PACKAGE
(TOP VIEW)

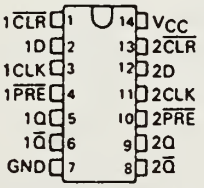

SN5474, SN54H74 . . . W PACKAGE
(TOP VIEW)

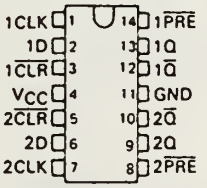

SN54LS74A, SN54S74 . . . FK PACKAGE
SN74LS74A, SN74S74 . . . FN PACKAGE
(TOP VIEW)

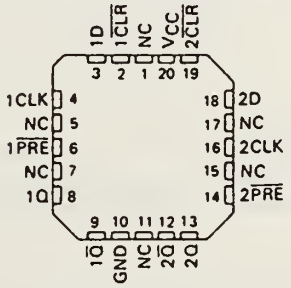

NC - No internal connection

logic diagram

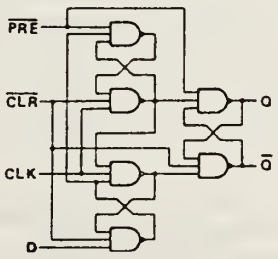

TYPES SN5400, SN54H00, SN54L00, SN54LS00, SN54S00, SN7400, SN74H00, SN74LS00, SN74S00 QUADRUPLE 2-INPUT POSITIVE-NAND GATES

REVISED DECEMBER 1983

- Package Options Include Both Plastic and Ceramic Chip Carriers in Addition to Plastic and Ceramic DIPs
- Dependable Texas Instruments Quality and Reliability

description

These devices contain four independent 2-input NAND gates.

The SN5400, SN54H00, SN54L00, and SN54LS00, and SN54S00 are characterized for operation over the full military temperature range of −55°C to 125°C. The SN7400, SN74H00, SN74LS00, and SN74S00 are characterized for operation from 0°C to 70°C.

FUNCTION TABLE (each gate)

INPUTS		OUTPUT
A	B	Y
H	H	L
L	X	H
X	L	H

logic diagram (each gate)

positive logic

$$Y = \overline{A \cdot B} \text{ or } Y = \overline{A} + \overline{B}$$

SN5400, SN54H00, SN54L00 . . . J PACKAGE
SN54LS00, SN54S00 . . . J OR W PACKAGE
SN7400, SN74H00 . . . J OR N PACKAGE
SN74LS00, SN74S00 . . . D, J OR N PACKAGE
(TOP VIEW)

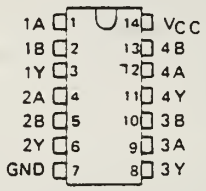

SN5400, SN54H00 . . . W PACKAGE
(TOP VIEW)

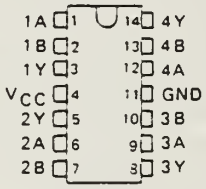

SN54LS00, SN54S00 . . . FK PACKAGE
SN74LS00, SN74S00 . . . FN PACKAGE
(TOP VIEW)

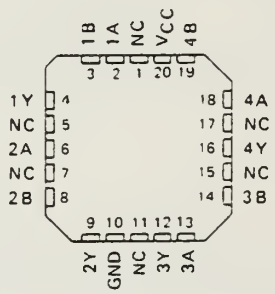

NC - No internal connection

PRODUCTION DATA
This document contains information current as of publication date. Products conform to specifications per the terms of Texas Instruments standard warranty. Production processing does not necessarily include testing of all parameters.

TEXAS INSTRUMENTS
POST OFFICE BOX 225012 • DALLAS, TEXAS 75265

TYPES SN54192, SN54193, SN54L192, SN54L193, SN54LS192, SN54LS193, SN74192, SN74193, SN74L192, SN74LS193 SYNCHRONOUS 4-BIT UP/DOWN COUNTERS (DUAL CLOCK WITH CLEAR)

DECEMBER 1972—REVISED DECEMBER 1983

- Cascading Circuitry Provided Internally
- Synchronous Operation
- Individual Preset to Each Flip-Flop
- Fully Independent Clear Input

TYPES	TYPICAL MAXIMUM COUNT FREQUENCY	TYPICAL POWER DISSIPATION
'192, '193	32 MHz	325 mW
'L192, 'L193	7 MHz	43 mW
'LS192, 'LS193	32 MHz	95 mW

SN54192, SN54193, SN54L192, SN54LS193 . . . J OR W PACKAGE
SN54L192, SN54L193 . . . J PACKAGE
SN74192, SN74193 . . . J OR N PACKAGE
SN74LS192, SN74LS193 . . . D, J OR N PACKAGE
(TOP VIEW)

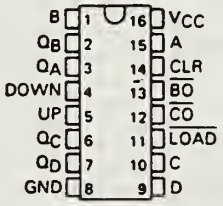

SN54LS192, SN54LS193 . . . FK PACKAGE
SN74LS192, SN74LS193 . . . FN PACKAGE
(TOP VIEW)

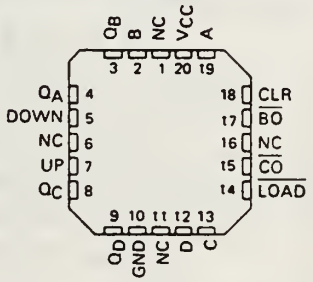

NC - No internal connection

description

These monolithic circuits are synchronous reversible (up/down) counters having a complexity of 55 equivalent gates. The '192, 'L192, and 'LS192 circuits are BCD counters and the '193, 'L193 and 'LS193 are 4-bit binary counters. Synchronous operation is provided by having all flip-flops clocked simultaneously so that the outputs change coincidently with each other when so instructed by the steering logic. This mode of operation eliminates the output counting spikes which are normally associated with asynchronous (ripple-clock) counters.

The outputs of the four master-slave flip-flops are triggered by a low-to-high-level transition of either count (clock) input. The direction of counting is determined by which count input is pulsed while the other count input is high.

All four counters are fully programmable; that is, each output may be preset to either level by entering the desired data at the data inputs while the load input is low. The output will change to agree with the data inputs independently of the count pulses. This feature allows the counters to be used as modulo-N dividers by simply modifying the count length with the preset inputs.

A clear input has been provided which forces all outputs to the low level when a high level is applied. The clear function is independent of the count and load inputs. The clear, count, and load inputs are buffered to lower the drive requirements. This reduces the number of clock drivers, etc., required for long words.

These counters were designed to be cascaded without the need for external circuitry. Both borrow and carry outputs are available to cascade both the up- and down-counting functions. The borrow output produces a pulse equal in width to the count-down input when the counter underflows. Similarly, the carry output produces a pulse equal in width to the count-up input when an overflow condition exists. The counters can then be easily cascaded by feeding the borrow and carry outputs to the count-down and count-up inputs respectively of the succeeding counter.

absolute maximum ratings over operating free-air temperature range (unless otherwise noted)

	SN54'	SN54L'	SN54LS'	SN74'	SN74LS'	UNIT
Supply voltage, V_{CC} (see Note 1)	7	8	7	7	7	V
Input voltage	5.5	5.5	7	5.5	7	V
Operating free-air temperature range	− 55 to 125			0 to 70		°C
Storage temperature range	− 65 to 150			− 65 to 150		°C

NOTE 1: Voltage values are with respect to network ground terminal.

PRODUCTION DATA
This document contains information current as of publication date. Products conform to specifications per the terms of Texas Instruments standard warranty. Production processing does not necessarily include testing of all parameters.

TEXAS INSTRUMENTS
POST OFFICE BOX 225012 • DALLAS, TEXAS 75265

National Semiconductor

DAC0808/DAC0807/DAC0806 8-Bit D/A Converters

General Description

The DAC0808 series is an 8-bit monolithic digital-to-analog converter (DAC) featuring a full scale output current settling time of 150 ns while dissipating only 33 mW with ±5V supplies. No reference current (I_{REF}) trimming is required for most applications since the full scale output current is typically ±1 LSB of 255 I_{REF}/ 256. Relative accuracies of better than ±0.19% assure 8-bit monotonicity and linearity while zero level output current of less than 4 μA provides 8-bit zero accuracy for $I_{REF} \geq 2$ mA. The power supply currents of the DAC0808 series are independent of bit codes, and exhibits essentially constant device characteristics over the entire supply voltage range.

The DAC0808 will interface directly with popular TTL, DTL or CMOS logic levels, and is a direct replacement for the MC1508/MC1408. For higher speed applications, see DAC0800 data sheet.

Features

- Relative accuracy: ±0.19% error maximum (DAC0808)
- Full scale current match: ±1 LSB typ
- 7 and 6-bit accuracy available (DAC0807, DAC0806)
- Fast settling time: 150 ns typ
- Noninverting digital inputs are TTL and CMOS compatible
- High speed multiplying input slew rate: 8 mA/μs
- Power supply voltage range: ±4.5V to ±18V
- Low power consumption: 33 mW @ ±5V

Block and Connection Diagrams

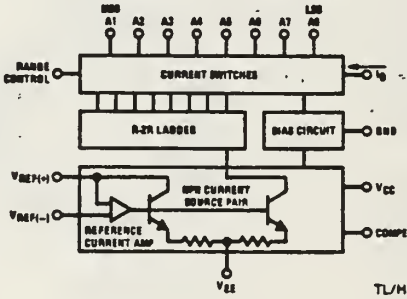

TL/H/5687–1

Order Number DAC0808, DAC0807, or DAC0806
See NS Package Number J16A, M16A or N16A

Dual-In-Line Package

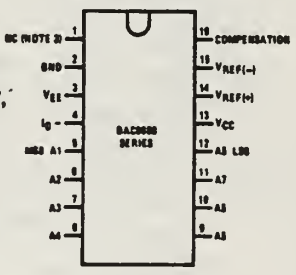

Top View

TL/H/5687–2

Small-Outline Package

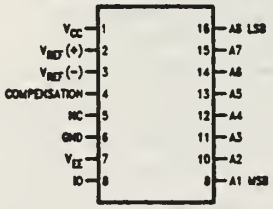

Top View

TL/H/5687–13

Ordering Information

ACCURACY	OPERATING TEMPERATURE RANGE	ORDER NUMBERS				
		J PACKAGE (J16A)*		N PACKAGE (N16A)*		SO PACKAGE (M16A)
8-bit	$-55°C \leq T_A \leq +125°C$	DAC0808LJ	MC1508L8			
8-bit	$0°C \leq T_A \leq +75°C$	DAC0808LCJ	MC1408L8	DAC0808LCN	MC1408P8	DAC0808LCM
7-bit	$0°C \leq T_A \leq +75°C$	DAC0807LCJ	MC1408L7	DAC0807LCN	MC1408P7	DAC0807LCM
6-bit	$0°C \leq T_A \leq +75°C$	DAC0806LCJ	MC1408L6	DAC0806LCN	MC1408P6	DAC0806LCM

*Note. Devices may be ordered by using either order number.

Absolute Maximum Ratings (Note 1)

If Military/Aerospace specified devices are required, please contact the National Semiconductor Sales Office/Distributors for availability and specifications.

Power Supply Voltage	
V_{CC}	+18 V_{DC}
V_{EE}	−18 V_{DC}
Digital Input Voltage, V5–V12	−10 V_{DC} to +18 V_{DC}
Applied Output Voltage, V_O	−11 V_{DC} to +18 V_{DC}
Reference Current, I_{14}	5 mA
Reference Amplifier Inputs, V14, V15	V_{CC}, V_{EE}
Power Dissipation (Note 3)	1000 mW
ESD Susceptibility (Note 4)	TBD
Storage Temperature Range	−65°C to +150°C
Lead Temp. (Soldering, 10 seconds)	
Dual-In-Line Package (Plastic)	260°C
Dual-In-Line Package (Ceramic)	300°C
Surface Mount Package	
Vapor Phase (60 seconds)	215°C
Infrared (15 seconds)	220°C

Operating Ratings

Temperature Range	$T_{MIN} \le T_A \le T_{MAX}$
DAC0808L	−55°C ≤ T_A ≤ +125°C
DAC0808LC Series	0 ≤ T_A ≤ +75°C

Electrical Characteristics

(V_{CC} = 5V, V_{EE} = −15 V_{DC}, V_{REF}/R14 = 2 mA, DAC0808: T_A = −55°C to +125°C, DAC0808C, DAC0807C, DAC0806C, T_A = 0°C to +75°C, and all digital inputs at high logic level unless otherwise noted.)

Symbol	Parameter	Conditions	Min	Typ	Max	Units
	Relative Accuracy (Error Relative to Full Scale I_O)	*(Figure 4)*				%
	DAC0808L (LM1508-8), DAC0808LC (LM1408-8)				±0.19	%
	DAC0807LC (LM1408-7), (Note 5)				±0.39	%
	DAC0806LC (LM1408-6), (Note 5)				±0.78	%
	Settling Time to Within ½ LSB (Includes t_{PLH})	T_A = 25°C (Note 6), *(Figure 5)*		150		ns
t_{PLH}, t_{PHL}	Propagation Delay Time	T_A = 25°C, *(Figure 5)*		30	100	ns
TC_O	Output Full Scale Current Drift			±20		ppm/°C
	Digital Input Logic Levels	*(Figure 3)*				
V_{IH}	High Level, Logic "1"		2			V_{DC}
V_{IL}	Low Level, Logic "0"				0.8	V_{DC}
	Digital Input Current	*(Figure 3)*				
	High Level	V_{IH} = 5V		0	0.040	mA
	Low Level	V_{IL} = 0.8V		−0.003	−0.8	mA
I_{REF}	Reference Input Bias Current	*(Figure 3)*		−1	−3	μA
	Output Current Range	*(Figure 3)*				
		V_{EE} = −5V	0	2.0	2.1	mA
		V_{EE} = −15V, T_A = 25°C	0	2.0	4.2	mA
	Output Current	V_{REF} = 2.000V, R14 = 1000Ω,				
		(Figure 3)	1.9	1.99	2.1	mA
	Output Current, All Bits Low	*(Figure 3)*		0	4	μA
	Output Voltage Compliance (Note 2)	E_r ≤ 0.19%, T_A = 25°C				
	V_{EE} = −5V, I_{REF} = 1 mA				−0.55, +0.4	V_{DC}
	V_{EE} Below −10V				−5.0, +0.4	V_{DC}

Electrical Characteristics (Continued)

(V_{CC} = 5V, V_{EE} = −15 V_{DC}, V_{REF}/R14 = 2 mA, DAC0808: T_A = −55°C to +125°C, DAC0808C, DAC0807C, DAC0806C: T_A = 0°C to +75°C, and all digital inputs at high logic level unless otherwise noted.)

Symbol	Parameter	Conditions	Min	Typ	Max
SRI_{REF}	Reference Current Slew Rate	*(Figure 6)*	4	8	
	Output Current Power Supply Sensitivity	$-5V \le V_{EE} \le -16.5V$		0.05	2.7
	Power Supply Current (All Bits Low)	*(Figure 3)*			
I_{CC}				2.3	22
I_{EE}				−4.3	−13
	Power Supply Voltage Range	T_A = 25°C, *(Figure 3)*			
V_{CC}			4.5	5.0	5.5
V_{EE}			−4.5	−15	−16.5
	Power Dissipation				
	All Bits Low	V_{CC} = 5V, V_{EE} = −5V		33	170
		V_{CC} = 5V, V_{EE} = −15V		106	305
	All Bits High	V_{CC} = 15V, V_{EE} = −5V		90	
		V_{CC} = 15V, V_{EE} = −15V		160	

Note 1: Absolute Maximum Ratings indicate limits beyond which damage to the device may occur. DC and AC electrical specifications do not apply when operating the device beyond its specified operating conditions.

Note 2: Range control is not required.

Note 3: The maximum power dissipation must be derated at elevated temperatures and is dictated by T_{JMAX}, θ_{JA}, and the ambient temperature, T_A. The maximum allowable power dissipation at any temperature is $P_D = (T_{JMAX} - T_A)/\theta_{JA}$ or the number given in the Absolute Maximum Ratings, whichever is lower. For the device, T_{JMAX} = 125°C, and the typical junction-to-ambient thermal resistance of the dual-in-line J package when the board mounted is 100°C/W. For the dual-in-line N package, this number increases to 175°C/W and for the small outline M package this number is 100°C/W.

Note 4: Human body model, 100 pF discharged through a 1.5 kΩ resistor.

Note 5: All current switches are tested to guarantee at least 50% of rated current.

Note 6: All bits switched.

Note 7: Pin-out numbers for the DAL080X represent the dual-in-line package. The small outline package pinout differs from the dual-in-line package.

Typical Application

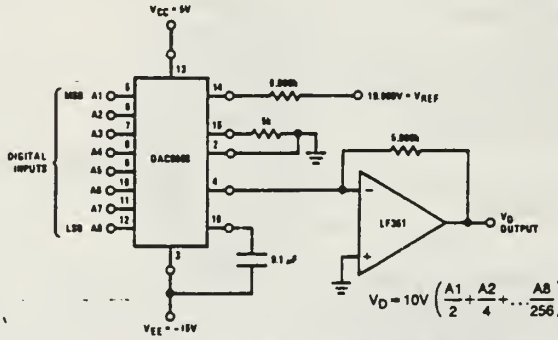

TL/H/5687–3

FIGURE 1. + 10V Output Digital to Analog Converter (Note 7)

APPENDIX M

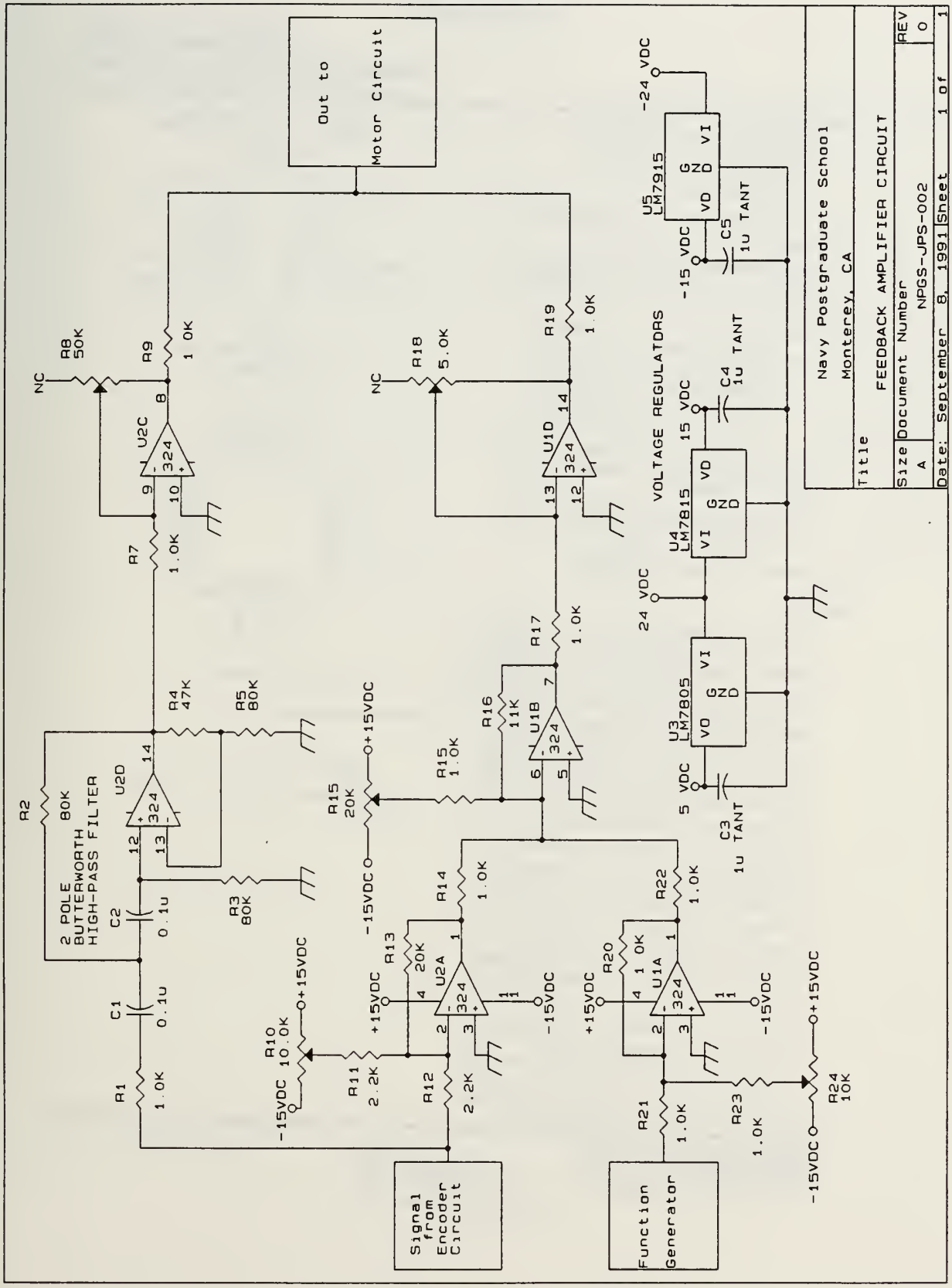
Out to Motor Circuit
Navy Postgraduate School
Monterey, CA
Title
FEEDBACK AMPLIFIER CIRCUIT
Size A
Document Number NPGS-JPS-002
REV 0
Date: September 8, 1991 Sheet 1 of 1
VOLTAGE REGULATORS
-24 VDC
-15 VDC
15 VDC
24 VDC
5 VDC
U5 LM7915
U4 LM7815
U3 LM7805
C5 1u TANT
C4 1u TANT
C3 1u TANT
2 POLE BUTTERWORTH HIGH-PASS FILTER
R2 80K
R4 47K
R5 80K
R3 80K
C2 0.1u
C1 0.1u
R1 1.0K
R8 50K
R9 1.0K
R7 1.0K
R18 5.0K
R19 1.0K
R17 1.0K
R16 11K
R15 1.0K
R15 20K
R14 1.0K
R13 20K
R11 2.2K
R12 2.2K
R10 10.0K
R22 1.0K
R20 1.0K
R21 1.0K
R23 1.0K
R24 10K
U2C
U2D
U1D
U1B
U2A
U1A
324
+15VDC
-15VDC
NC
Signal from Encoder Circuit
Function Generator

LM124, LM224, LM224A, LM324, LM324A, LM2902 QUADRUPLE OPERATIONAL AMPLIFIERS

D1990, SEPTEMBER 1975—REVISED JANUARY 1989

- Wide Range of Supply Voltages:
  Single Supply . . . 3 V to 30 V
  (LM2902 . . . 3 V to 26 V),
  or Dual Supplies
- Low Supply Current Drain Independent of Supply Voltage . . . 0.8 mA Typ
- Common-Mode Input Voltage Range Includes Ground Allowing Direct Sensing near Ground
- Low Input Bias and Offset Parameters:
  Input Offset Voltage . . . 3 mV Typ
  A Versions . . . 2 mV Typ
  Input Offset Current . . . 2 nA Typ
  Input Bias Current . . . 20 nA Typ
  A Versions . . . 15 nA Typ
- Differential Input Voltage Range Equal to Maximum-Rated Supply Voltage . . . 32 V (26 V for LM2902)
- Open-Loop Differential Voltage Amplification . . . 100 V/mV Typ
- Internal Frequency Compensation

LM124 . . . J OR W PACKAGE
ALL OTHERS . . . D, J, OR N PACKAGES
(TOP VIEW)

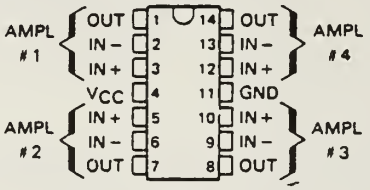

LM124
FK CHIP CARRIER PACKAGE
(TOP VIEW)

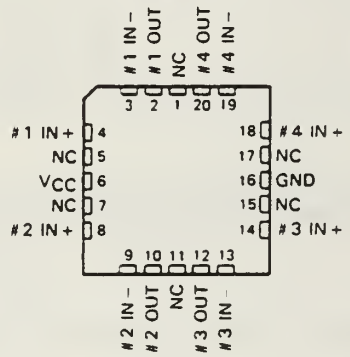

NC—No internal connection

description

These devices consist of four independent, high-gain frequency-compensated operational amplifiers that were designed specifically to operate from a single supply over a wide range of voltages. Operation from split supplies is also possible so long as the difference between the two supplies is 3 V to 30 V (for the LM2902, 3 V to 26 V), and Pin 4 is at least 1.5 V more positive then the input common-mode voltage. The low supply current drain is independent of the magnitude of the supply voltage.

Applications include transducer amplifiers, d-c amplification blocks, and all the conventional operational amplifier circuits that now can be more easily implemented in single-supply-voltage systems. For example, the LM124 can be operated directly off of the standard 5-V supply that is used in digital systems and will easily provide the required interface electronics without requiring additional ±15-V supplies.

The LM124 is characterized for operation over the full military temperature range of −55°C to 125°C. The LM2902 is characterized for operation from −40°C to 105°C, the LM224 and LM224A from −25°C to 85°C, and the LM324 and LM324A from 0°C to 70°C.

symbol (each amplifier)

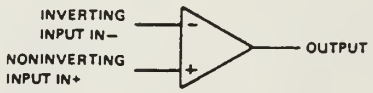

PRODUCTION DATA documents contain information current as of publication date. Products conform to specifications per the terms of Texas Instruments standard warranty. Production processing does not necessarily include testing of all parameters.

Copyright © 1979, Texas Instruments Incorporated

APPENDIX O

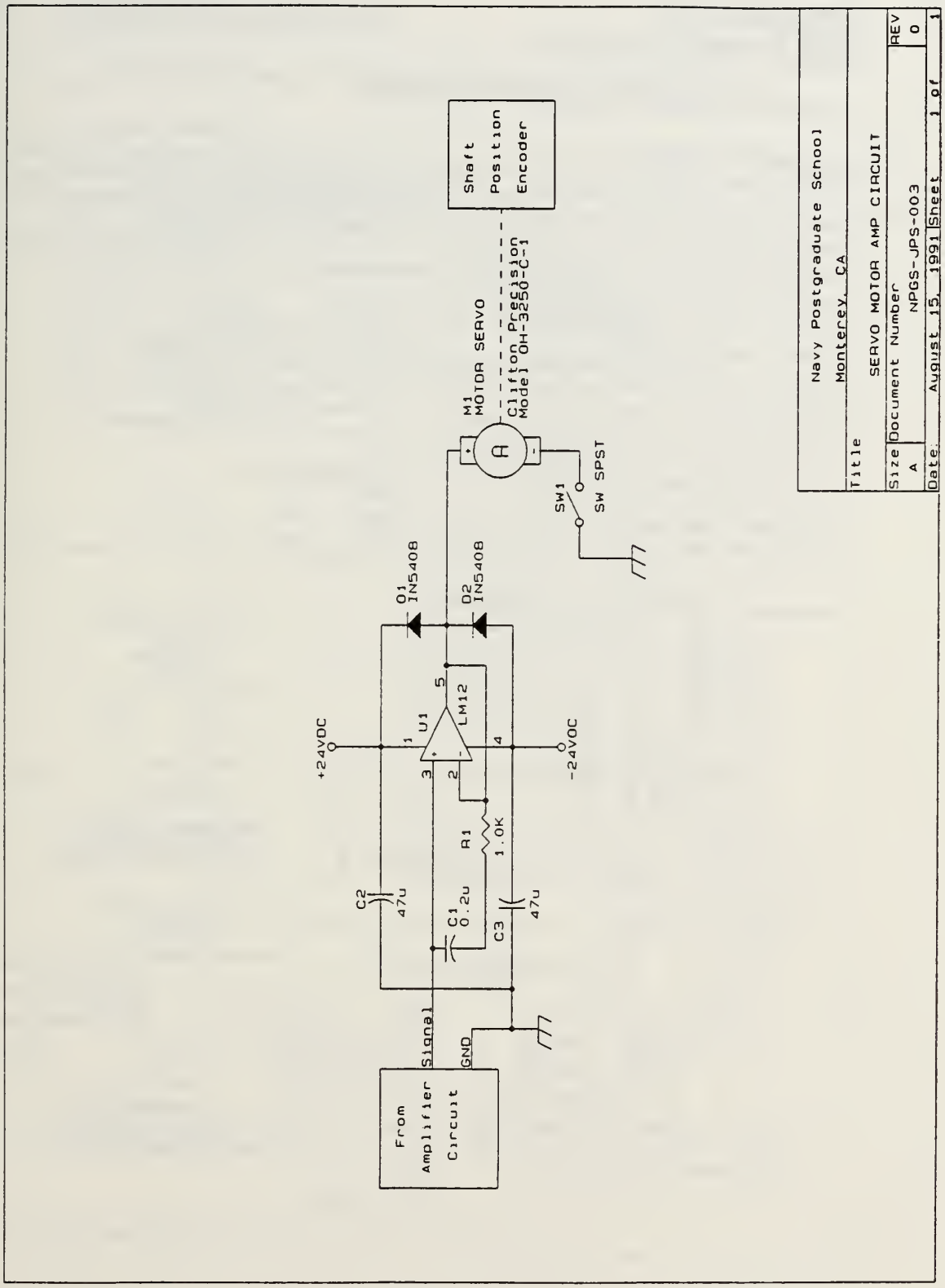
Navy Postgraduate School
Monterey, CA
Title
SERVO MOTOR AMP CIRCUIT
Size
A
Document Number
NPGS-JPS-003
REV
0
Date: August 15, 1991 Sheet 1 of 1
Shaft
Position
Encoder
M1
MOTOR SERVO
Clifton Precision
Model OH-3250-C-1
SW1
SW SPST
D1
IN5408
D2
IN5408
+24VDC
-24VDC
U1
LM12
R1
1.0K
C1
0.2u
C2
47u
C3
47u
From
Amplifier
Circuit
Signal
GND

National Semiconductor

LM78XX Series Voltage Regulators

General Description

The LM78XX series of three terminal regulators is available with several fixed output voltages making them useful in a wide range of applications. One of these is local on card regulation, eliminating the distribution problems associated with single point regulation. The voltages available allow these regulators to be used in logic systems, instrumentation, HiFi, and other solid state electronic equipment. Although designed primarily as fixed voltage regulators these devices can be used with external components to obtain adjustable voltages and currents.

The LM78XX series is available in an aluminum TO-3 package which will allow over 1.0A load current if adequate heat sinking is provided. Current limiting is included to limit the peak output current to a safe value. Safe area protection for the output transistor is provided to limit internal power dissipation. If internal power dissipation becomes too high for the heat sinking provided, the thermal shutdown circuit takes over preventing the IC from overheating.

Considerable effort was expanded to make the LM78XX series of regulators easy to use and minimize the number of external components. It is not necessary to bypass the output, although this does improve transient response. Input bypassing is needed only if the regulator is located far from the filter capacitor of the power supply.

For output voltage other than 5V, 12V and 15V the LM117 series provides an output voltage range from 1.2V to 57V.

Features

- Output current in excess of 1A
- Internal thermal overload protection
- No external components required
- Output transistor safe area protection
- Internal short circuit current limit
- Available in the aluminum TO-3 package

Voltage Range

LM7805C	5V
LM7812C	12V
LM7815C	15V

Schematic and Connection Diagrams

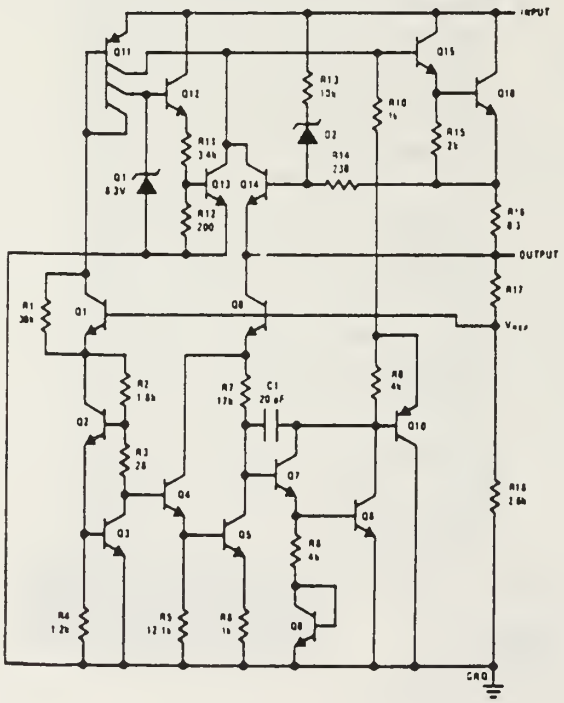

TL/H/7746–1

Metal Can Package
TO-3 (K)
Aluminum

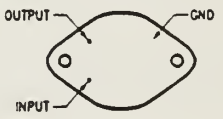

TL/H/7746–2

Bottom View

Order Number LM7805CK,
LM7812CK or LM7815CK
See NS Package Number KC02A

Plastic Package
TO-220 (T)

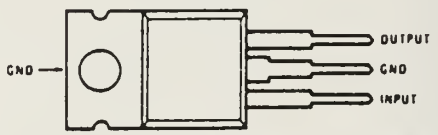

TL/H/7746–3

Top View

Order Number LM7805CT,
LM7812CT or LM7815CT
See NS Package Number T03B

National Semiconductor

LM79XX Series 3-Terminal Negative Regulators

General Description

The LM79XX series of 3-terminal regulators is available with fixed output voltages of −5V, −12V, and −15V. These devices need only one external component—a compensation capacitor at the output. The LM79XX series is packaged in the TO-220 power package and is capable of supplying 1.5A of output current.

These regulators employ internal current limiting safe area protection and thermal shutdown for protection against virtually all overload conditions.

Low ground pin current of the LM79XX series allows output voltage to be easily boosted above the preset value with a resistor divider. The low quiescent current drain of these devices with a specified maximum change with line and load ensures good regulation in the voltage boosted mode.

For applications requiring other voltages, see LM137 data sheet.

Features

- Thermal, short circuit and safe area protection
- High ripple rejection
- 1.5A output current
- 4% preset output voltage

Typical Applications

± 15V, 1 Amp Tracking Regulators

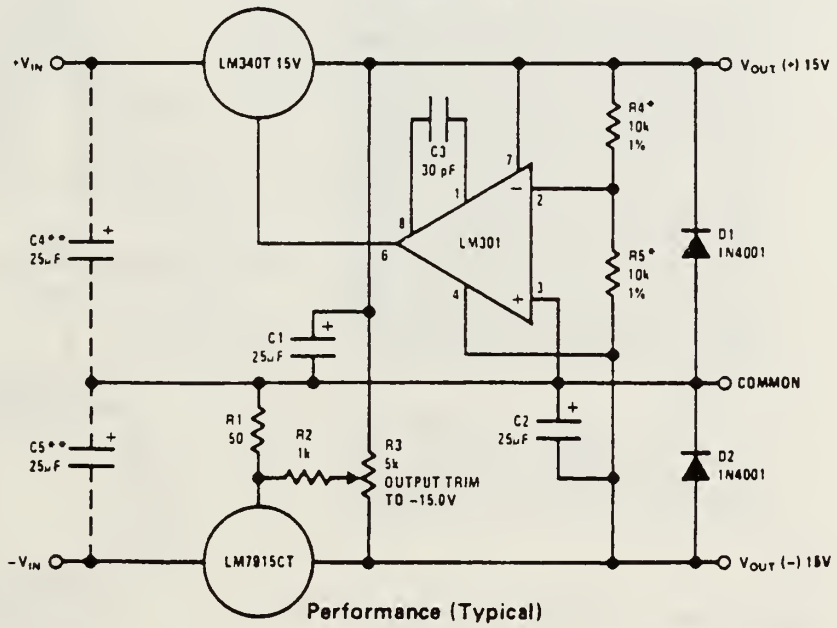

Performance (Typical)

TL/H/7340–1

	(−15)	(+15)
Load Regulation at ΔI_L = 1A	40 mV	2 mV
Output Ripple, C_{IN} = 3000 μF, I_L = 1A	100 μVrms	100 μVrms
Temperature Stability	50 mV	50 mV
Output Noise 10 Hz ≤ f ≤ 10 kHz	150 μVrms	150 μVrms

*Resistor tolerance of R4 and R5 determine matching of (+) and (−) outputs.

**Necessary only if raw supply filter capacitors are more than 3" from regulators.

LM101A, LM201A, LM301A
HIGH-PERFORMANCE OPERATIONAL AMPLIFIERS

D961, OCTOBER 1979—REVISED JUNE 1988

- Low Input Currents
- Low Input Offset Parameters
- Frequency and Transient Response Characteristics Adjustable
- Short-Circuit Protection
- Offset-Voltage Null Capability
- No Latch-Up
- Wide Common-Mode and Differential Voltage Ranges
- Same Pin Assignments as uA709
- Designed to be Interchangeable with National Semiconductor LM101A and LM301A

D, JG, OR P PACKAGE
(TOP VIEW)

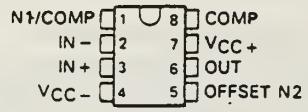

LM101A
W FLAT PACKAGE
(TOP VIEW)

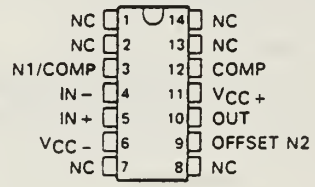

LM101A
U FLAT PACKAGE
(TOP VIEW)

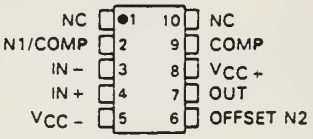

LM101A
FK CHIP-CARRIER PACKAGE
(TOP VIEW)

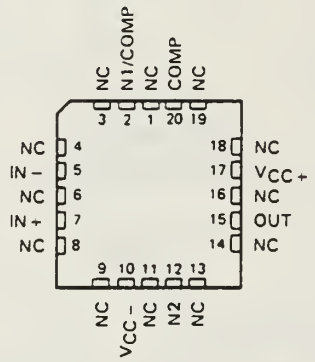

NC – No internal connection

description

The LM101A, LM201A, and LM301A are high-performance operational amplifiers featuring very low input bias current and input offset voltage and current to improve the accuracy of high-impedance circuits using these devices. The high common-mode input voltage range and the absence of latch-up make these amplifiers ideal for voltage-follower applications. The devices are protected to withstand short circuits at the output. The external compensation of these amplifiers allows the changing of the frequency response (when the closed-loop gain is greater than unity) for applications requiring wider bandwidth or higher slew rate. A potentiometer may be connected between the offset-null inputs (N1 and N2), as shown in Figure 7, to null out the offset voltage.

The LM101A is characterized for operation over the full military temperature range of −55°C to 125°C, the LM201A is characterized for operation from −25°C to 85°C, and the LM301A is characterized for operation from 0°C to 70°C.

symbol

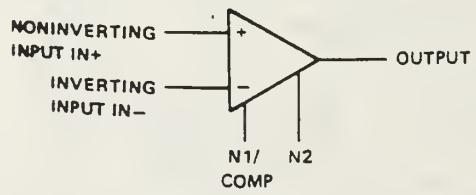

PRODUCTION DATA documents contain information current as of publication date. Products conform to specifications per the terms of Texas Instruments standard warranty. Production processing does not necessarily include testing of all parameters.

Copyright © 1983 Texas Instruments Incorporated

APPENDIX B

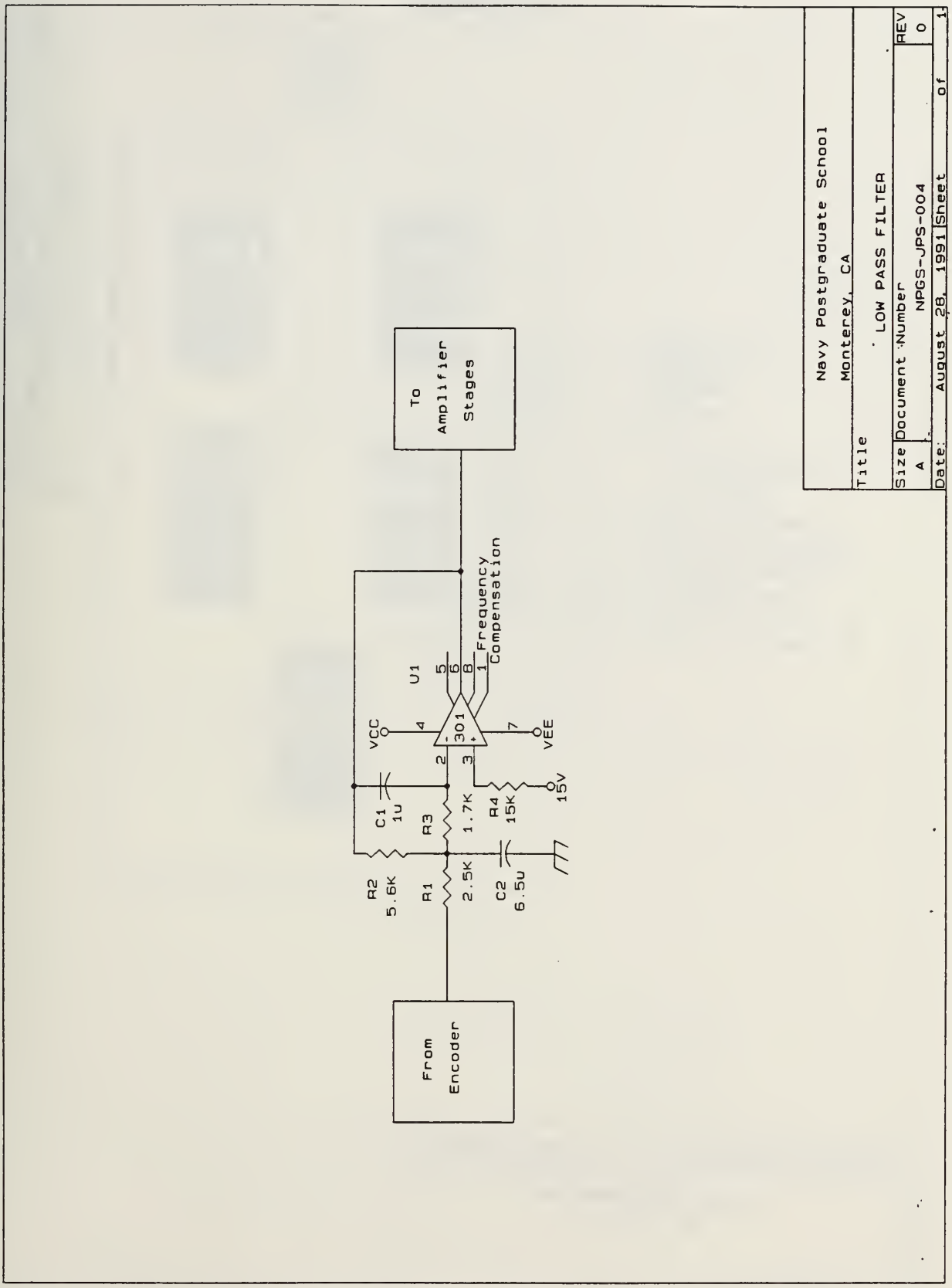
To
Amplifier
Stages
U1
5
6
8
1
Frequency
Compensation
VCC
4
301
7
VEE
2
3
C1
1u
R3
1.7K
R4
15K
15V
R2
5.6K
R1
2.5K
C2
6.5u
From
Encoder
Navy Postgraduate School
Monterey, CA
Title
LOW PASS FILTER
Size
A
Document Number
NPGS-JPS-004
REV
0
Date:
August 28, 1991
Sheet
of

APPENDIX T

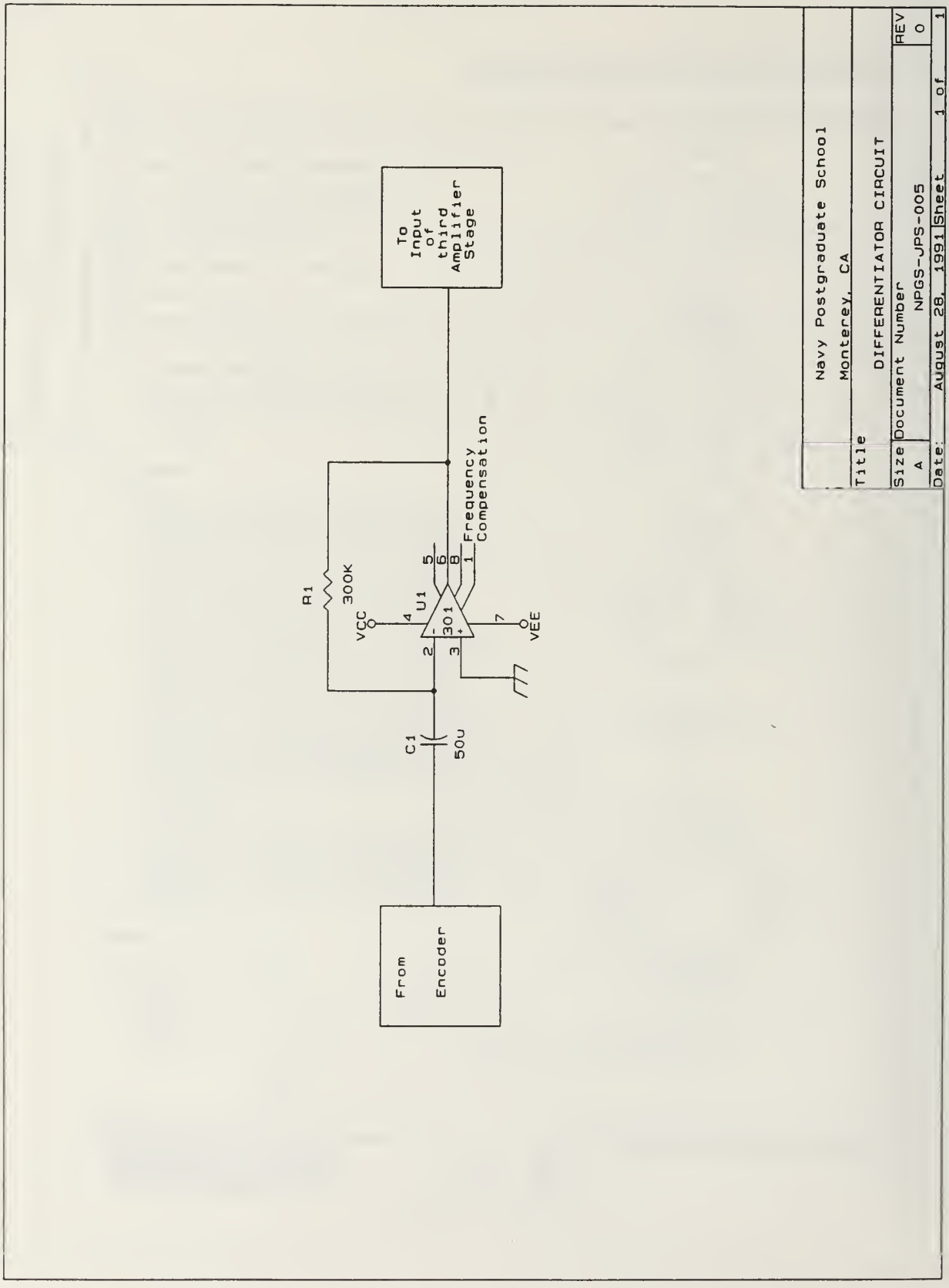
To Input of third Amplifier Stage
Frequency Compensation
R1
300K
VCC
U1
301
VEE
C1
50u
From Encoder
Navy Postgraduate School
Monterey, CA
Title
DIFFERENTIATOR CIRCUIT
Size
A
Document Number
NPGS-JPS-005
REV
0
Date:
August 28, 1991
Sheet
1 of 1

APPENDIX U

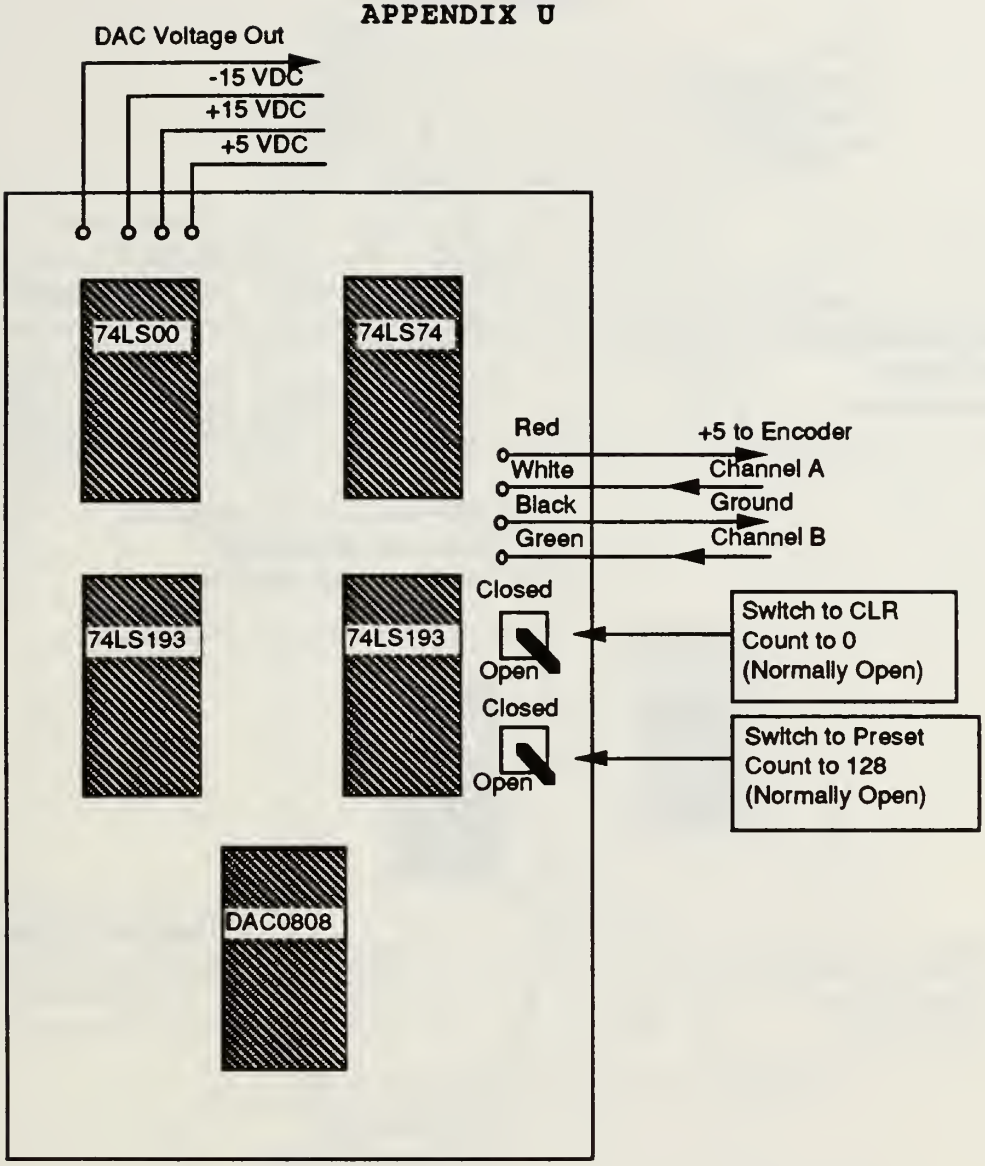

ENCODER-ANALOG CARD PARTS LOCATION
Navy Postgraduate School Monterey, CA J. P. Sargent 9-9-91

APPENDIX V

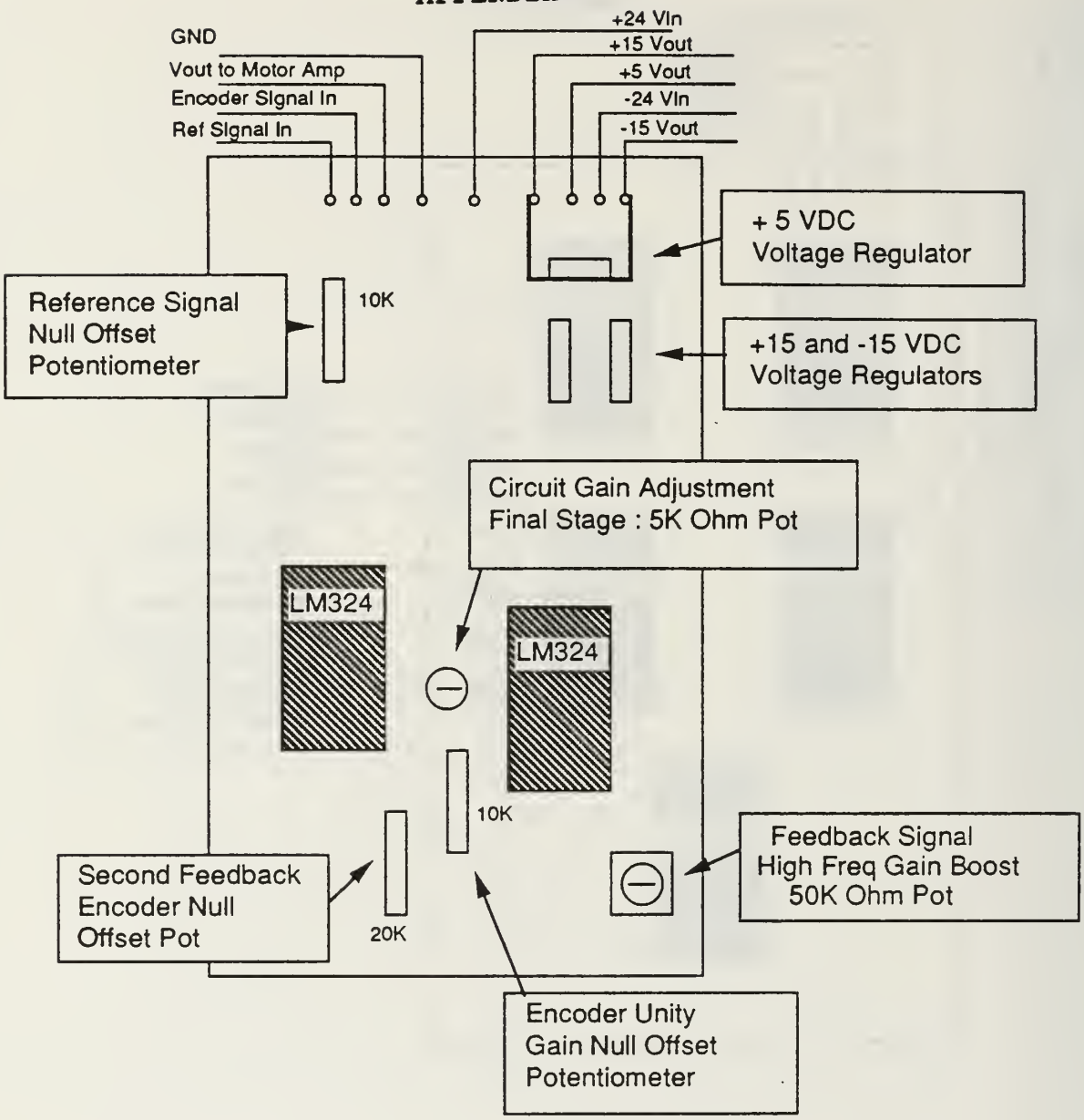

AMPLIFIER CARD PARTS LOCATION
Navy Postgraduate School Monterey, CA J. P. Sargent 9-9-91

APPENDIX W

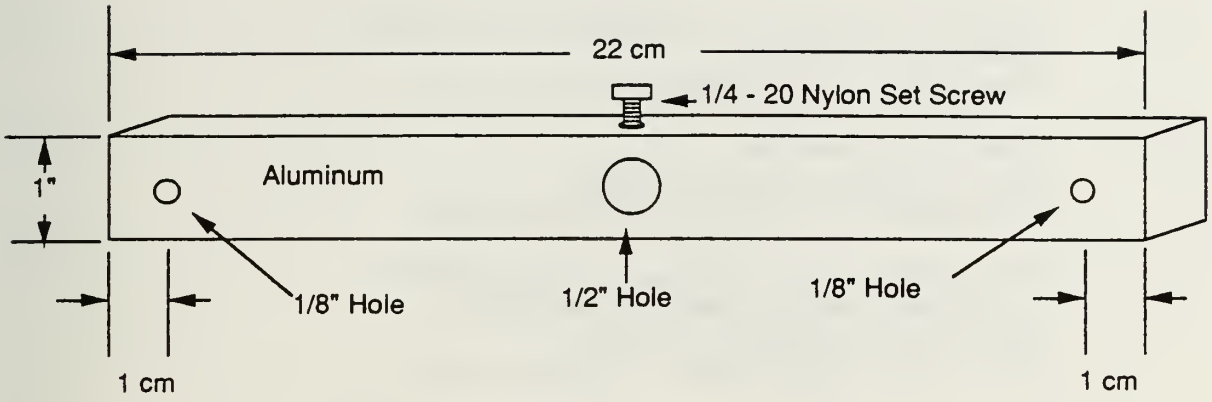

TORQUE TEST BAR

Navy Postgraduate School
Monterey, CA

J. P. Sargent 9-9-91

INITIAL DISTRIBUTION LIST

1.	Defense Technical Information Center Cameron Station Alexandria, Virginia 22304-6145	2
2.	Library, Code 52 Naval Postgraduate School Monterey, California 93943-5002	2
3.	Professor K.E. Woehler, Code PH/Wh Chairman, Department of Physics Naval Postgraduate School Monterey, California 93943-5000	1
4.	Assoc. Professor D.S. Davis, Code PH/Dv Department of Physics Naval Postgraduate School Monterey, California 93943-5000	2
5.	Assoc. Professor D.L. Walters, Code PH/We Department of Physics Naval Postgraduate School Monterey, California 93943-5000	1
6.	Department of Physics Library Naval Postgraduate School Monterey, California 93943-5000	2
7.	Commandant (G-ER) U. S. Coast Guard Headquarters 2100 Second St. S.W. Washington, D.C. 20593-0001	1
8.	LT. J.P. Sargent, USCG U. S. Coast Guard Research and Development Center Avery Point Groton, Connecticut 06340-6096	2

Thesis
S16672
c.1

Sargent
A design, fabrication and test of a precision positioning servo drive for a multiplexed imaging system.

Thesis
S16672
c.1

Sargent
A design, fabrication and test of a precision positioning servo drive for a multiplexed imaging system.

AMERICAN BINDERY 2 9-93

DUDLEY KNOX LIBRARY
3 2768 00018535 9